Water vapor budget of cold surge vortices

by

Jenq-Dar Tsay

A thesis submitted to the graduate faculty

in partial fulfillment of the requirements for the degree of

MASTER OF SCIENCE

Major: Meteorology

Program of Study Committee:
Tsing-Chang Chen, Major Professor
William A. Gallus, Jr.
S. Elwynn Taylor

Iowa State University

Ames, Iowa

2004

Graduate College
Iowa State University

This is to certify that the master's thesis of

Jenq-Dar Tsay

has met the thesis requirements of Iowa State University

Signatures have been redacted for privacy

TABLE OF CONTENTS

LIST OF FIGURES

ABSTRACT

The rainy season in Southeast Asia takes place during the northern winter. Cold surge vortices, which are initiated by cold surge events in East Asia, contribute over the half amount of precipitation in Southeast Asia and become the major source of rainfall.

In this study, the water vapor budget analysis shows that the convergence of water vapor flux associated with cold surge vortices is generally strong. It not only transports the moisture into Southeast Asia, but also regulates the life cycle of a cold surge vortex. In addition, the interannual variation of the occurrence frequency of cold surge vortices can affect the total amount of the convergence of water vapor flux, which in turn results in the interannual variation of precipitation over Southeast Asia.

Cold surge vortices can intensify the Southeast Asian high, the major circulation of the Asian winter monsoon, maintained by the Sverdrup balance. Results indicate that the maintenance of the anomalous circulation cannot be fully explained by the Sverdrup balance. The convergence of the eddy vorticity flux through the total transient flow contributed by cold surge vortex is required to maintain the anomalous circulation during cold surge vortices activity. The streamfunction budget analysis shows that the transient vorticity flux reinforces the vortex stretching effect to counter-balance the advection of planetary vorticity and helps to maintain the upper-level circulation anomalies.

CHAPTER 1. GENERAL INTRODUCTION

1.1 Introduction

Soybeans and corn are the world's leading source of protein and oil. Iowa ranks number one in the U.S. for both soybeans and corn product*. Meanwhile, the Southeast Asian countries became the world's fastest developing countries in the last decade; long-term economic forces in Southeast Asia have led to a sharp increase in U.S. agricultural exports to this region. It provides increased opportunities for U.S. trade**. Therefore, a better understanding of the Southeast Asia climate can help manage the agricultural economy in Iowa.

Southeast Asia highly depends on the monsoon rainfall, and the variability in the onset and the duration of monsoon has a profound impact on agriculture, water resources, and ecosystems (Pittock et al. 2001). Using climatology data collected by Braak (1921-1929) and Preedy (1966), Ramage (1971) examined the annual variation of the precipitation over Southeast Asia and found that maximum rainfall occurs during winter (December to February). According to Global Historical Climatological Network (GHCN) station data in Southeast Asia (Fig.1.1a), maximum rainfall around Malaysia and Sumatra, Indonesia appears during the winter (Figs.1.1b, 1.1c, and 1.1d).

Ramage (1954) identified two types of tropical disturbances that bring rain to normally dry Southeast Asia during the cool season (November – April). Later, Cheang (1977) classified four types of synoptic conditions that can induce huge amounts of precipitation over Malaysia during winter. Three of them are related to the near-equator disturbances,

---

* A look at Iowa Agriculture, *Iowa Agriculture in the Classroom/USDA*

** Ag Trade Opportunities in Southeast Asia, *Economics Research Service/USDA*, Nov, 1997

while two of these three near-equator disturbances are related to conditions that could cause widespread torrential rainfall. Hence, the near-equator disturbances in Southeast Asia were noticed.

The Winter Monsoon Experiment (WMONEX) during the period from December 1, 1978, to March 5, 1979, was conducted to understand the East Asian winter monsoon and the role of the East Asian winter monsoon in large-scale atmospheric circulation. The precipitation over Southeast Asia, associated with the northeasterly Asian monsoon, was also one of the major research themes in the WMONEX.

In the pre-MONEX study, Chang et al. (1979) used data from the first half of December 1974 to study near-tropical disturbances, the possible relationship between the East Asian cold surge, and the near-tropical cumulus convection system. They pointed out that a cold surge from East Asia can enhance a low-level convergence and organized deep cumulus convection over Southeast Asia. The associated heavy convective precipitation and the released latent heat form one of the major heat sources of global circulation. In another pre-MONEX study, Chang and Lau (1980) investigated the change of Hadley-type and Walker-type circulations and found that they were related to cold surges during December 1974. They indicated that cold surge events in East Asia are capable of enhancing the local Hadley circulation and the tropical east-west circulation. Accordingly, cold surge related deep cumulus convection in Southeast Asia is a crucial feature in strengthening Hadley and Walker circulations

During the MONEX, three former Soviet Union's observation ships were located in the southern part of the South China Sea, and a radar unit from the Massachusetts Institute of Technology (MIT) was located on the coast of Borneo. The data collected by these ships

were analyzed by different groups to understand the structure of the cold surge related near-equator cumulus convection. Johnson (1981) reported that convective activity could be modulated by a long-period synoptic force (e.g. monsoon surges, easterly wave). Using the radar data, Houze et al. (1981) described the structure and temporal variation of the clouds and precipitation and pointed out that the diurnal cycle of the convective activity is caused by the interaction between the monsoon surge and the land-sea breeze on the west coast of Borneo. Later, Johnson and Kriete (1982) used the rawinsonde data from the three Soviet ships to compute the vertical motion inside the convection. The peak vertical motion was located near 250mb. The detailed thermodynamic structure and circulation features of this mesoscale cloud system and the feature in the near environment were later summarized by Johnson (1982).

A possible relationship between the anomalous Walker circulation, Hadley circulation and the sea surface temperature, which form the well known El Niño / Southern Oscillation (ENSO), was suggested by Bjerknes (1969). Brakk (1919) found the rainfall anomalies over Indonesia during the wet season are related to the surface pressure over northern Australia. Berlage (1927) suggested that rainfall over Java is lag-correlated with Darwin pressure, with the latter leading by about one season; both are related to the southern oscillation. Their relationships have received support from the study done by Nicholls (1981).

The major upward motion branch of the global circulation is located nearby in Southeast Asia. During the 1982 to 1983 ENSO, Indonesia faced the worst drought in the 20th century. Many other regions of the world were also similarly affected by either drought or flood conditions (Rasmusson and Carpenter 1983, Simmon and Wallace 1983). The distribution of the anomalies circulation along the equator can be interpreted as the

presence of the Walker circulation in the reverse sense, with rising motions over the equatorial central Pacific and Indian Oceans and a sinking motion over the "maritime continent" (Ramage 1968). Winter monsoon activities over the East Asian sector during the 1982 to 1983 ENSO event were much reduced because of the suppression of the Indonesian convection (Lau and Chang 1987).

Chen (2002a) showed that the occurrence frequency of cold surge vortices for the 1979-1999 period (Fig.1.2a) have a clear interannual variation with the sea surface temperature anomalies over the NOAA NINO3.4 area (170°W-120°W, 5°S~5°N). During the cold ENSO phase [cold (warm) ENSO phase defined by anomalous sea surface temperatures (SST) lower (higer) than 0.5 degree over the NINO3.4 region], the interaction between cold-air outflow from East Asia, and tropical cyclonic flows can (Fig.1.2c) form a low-level environment favorable to the occurrence frequency of cold surge vortices over northeast Indian Ocean, south of South China Sea, Philippine Sea (Fig.1.2c). In contrast, the reversed situation occurs during the warm ENSO phase (Fig.1.2b). It was pointed out by Cheang (1987) that cold surge vortices could contribute over one-half amount of the precipitation in Malaysia during a winter season. If the occurrence frequency of cold surge vortex has a clear interannual variation associated with the ENSO events, it may play a major role in the interannual variation of precipitation in Southeast Asia. Possibly, cold surge vortices are the regional weather phenomena in response to large-scale circulation affected by the ENSO which in turn modulate the regional precipitation. In order to assess the contribution of the interannual variation of cold surge vortices occurrence frequency to the interannual variation of the precipitation over Southeast Asia, this study will conduct a comprehensive study of the water vapor budget of cold surge vortices.

Previous studies (Lau and Chang 1987, Yen and Chen 2002) demonstrated that the tropical convection enhanced by the East Asian cold surge can intensify the local Hadley Cell and accelerate the East Asian Jet, which is also a result of the interaction between the Southeast Asian high and the East Asian trough (Chen and Yen et al. 2002). The deep cumulus convection associated with cold surge vortex over Southeast Asia releases a large amount of heat into the atmosphere. The diabatic heating formed by this process is a major driving force of the winter atmosphere circulation over Southeast Asia. To understand the role of cold surge vortices in the large-scale circulation, the streamfunction budget analysis is applied in the study.

1.2 Thesis Organization

This study consists of seven chapters. An overview of the methodology and data used in this study is presented in Chapter 2. The climatology of Southeast Asia's water vapor budget and circulation is provided in Chapter 3. The life cycle of cold surge vortex case and the water vapor budget analysis to portray the character of their hydrological cycle are illustrated in Chapter 4. The interannual variation of cold surge vortex activity and the impact on the precipitation over Southeast Asia are shown in Chapter 5. The role of cold surge vortex in the large-scale circulation through a streamfunction budget analysis is discussed in Chapter 6. Finally, a summary of the results is offered in Chapter 7.

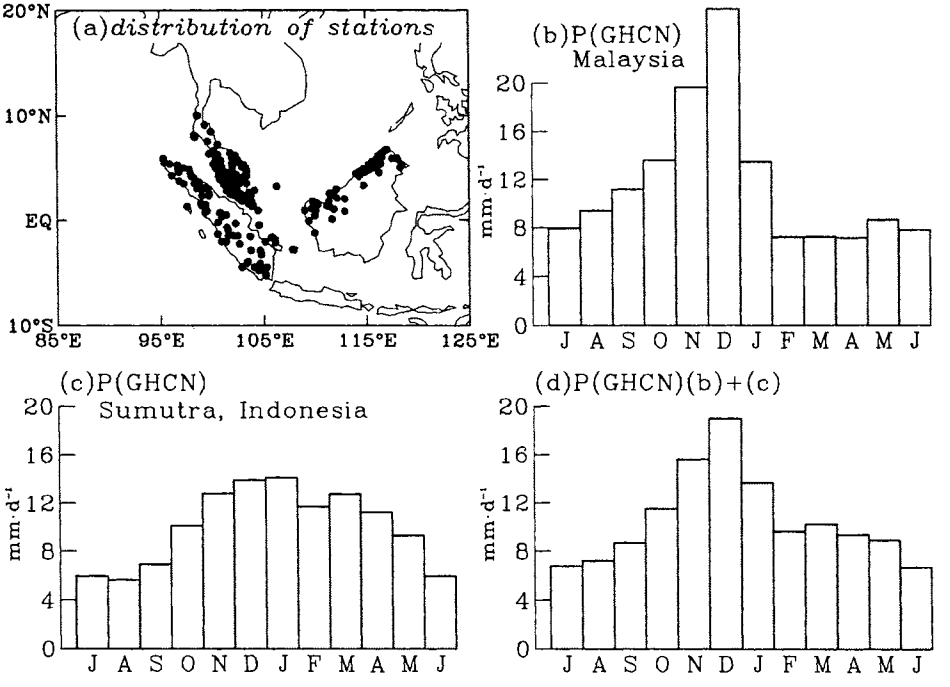

Fig.1.1 (a) Distribution of the observation stations over Malaysia and Sumatra, Indonesia. (b) Histogram of the annual precipitation over Malaysia. (c) Histogram of annual precipitation over Sumatra, Indonesia. (d) Histogram of annual precipitation over Malaysia and Sumatra, Indonesia.

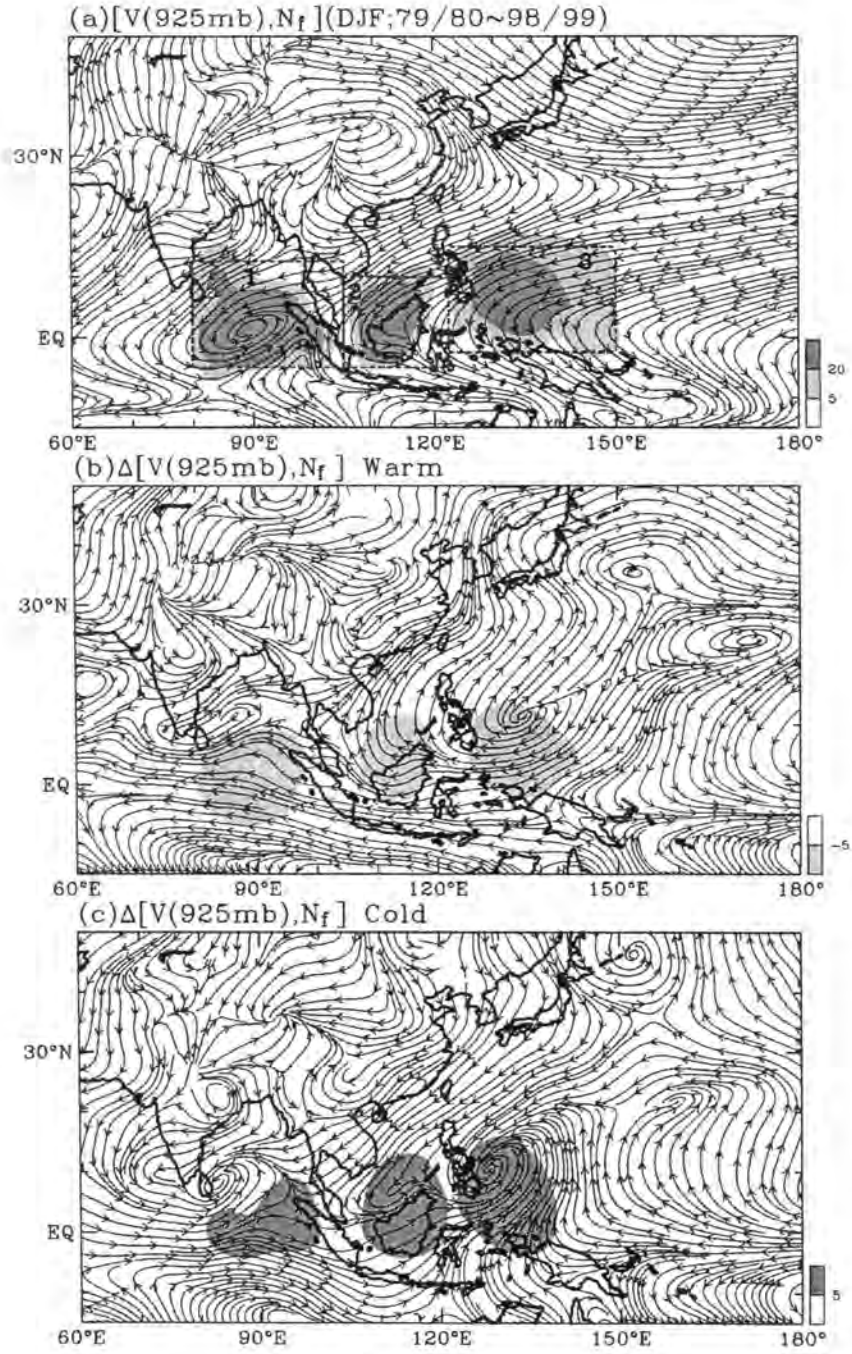

Fig.1.2 (a) The occurrence frequency (N_f) of cold surge vortices in southeast and south Asia superimposed on the 925mb streamline: (a) climatology of 1979-99, (b) composite departures for all warm ENSO winters, and (c) composite departures for all cold ENSO winters [adopted from Chen (2002a)].

CHAPTER 2. DATA AND METHODOLOGY

This chapter consists of a description of the data and methodology used in this study. It highlights three major topics: 1) data sources, 2) the water vapor budget, and 3) the streamfunction budget analysis.

2.1 Data sources

2.1.1 NCEP Reanalysis II

The first version of the National Center for Environment Prediction (NCEP) Reanalysis (R-1) was introduced by Kalnay et al. (1996). The second version of the NCEP Reanalysis (R-2), which corrected report's error was introduced by Kanamitsu et al. (2002). The data resolution is 2.5° (latitude) ×2.5° (longitude) in the horizontal resolution with 17 levels in the vertical resolution; only the 12 lower levels (1000, 925, 850, 700, 600, 500, 400, 300, 250, 200, 150, 100mb) are used in this study. More detail and explanation can be found in Kalnay et al. (1996) and Kanamitsu et al. (2002)'s study.

2.1.2 Precipitation Data

2.1.2.1 Goddard Precipitation Index (GPI)

The estimated precipitation generated from Television Infrared Observation Satellite (TIROS) Operation Vertical Sounder (TVOS) Pathfinder Path A are used (hereafter GPI) (Susskind et al. 1997). The GPI is derived from the analysis of High resolution Infrared Radiation (HIRS2) and Microwave Sounding Unit (MSU) observations on board the National Oceanic and Atmospheric Administration (NOAA) polar orbiting operational meteorological satellite. The horizontal resolution is a 1.0° (latitude) ×1.0° (longitude) gridded, averaging the 'fly-by' pixel observation. The GPI is available during (1979~1980

and 1988~1997), so that the gap is filled by the precipitation generated by the NCEP reanalysis II and compared with the outgoing longwave radiation (OLR) data.

2.1.2.2 Global Historical Climatological Network (GHCN)

The Global Historical Climatalogical Network (GHCN) is a global surface climate data set. It is comprised of surface station precipitation, temperature, and pressure data compiled on a monthly basis. There are two versions of the GHCN data, version 1 and 2. Since version 2 includes more station data and has a better quality control and homogeneity among measurements, it was used in this study to verify the interannual variation of the precipitation of the Southeast Asia. GHCN data is a joint project by the National Climatic Data Center, Arizona State University, and the Carbon Dioxide Information Analysis Center at Oak Ridge National Laboratory. For more information about GHCN station precipitation data, see Vose et al. (1992) and Easterling et al. (1996).

2.1.3 Outgoing long wave radiation from NOAA (OLR)

Interpolated OLR data are provided by the NOAA-CIRES (Cooperative Institute for Research in Environmental Sciences) Climate Diagnostic Center in Boulder, Colorado, from their web site at http://www.cdc.noaa.gov/. The data were derived from the twice daily Advanced Very High Resolution Radiometer (AVHRR) soundings for OLR. Monthly mean values were then calculated. The horizontal dimension of the data is 144 × 73, which translates to 2.5° (latitude) × 2.5° (longitude) grid spacing. OLR can provided a rough estimate of the precipitation intensity. In this study, OLR was used to verify the GPI and the precipitation produced by NCEP Reanalysis II.

2.2 Methodology

2.2.1 Water vapor budget

A study of the moisture transport over the Northern Hemisphere was made by Starr and his colleagues at the Massachusetts Institute of Technology (MIT) under the planetary circulation project (Starr and Saltzman 1996). Starr's colleagues, including Rasmusson (1972), Rosen et al.(1979a), Peixoto et al. (1981), Salstein et al. (1980), and Peixoto and Oort (1983), carried the research on this subject further. The formulation of the atmospheric branch of the hydrological cycle is based on the balance requirement of water vapor in the atmosphere. This study will follow the general discussions of water vapor budget from Peixoto and Oort (1983, 1991).

Without any phase change, the formulation of the water balance can be simplified as

$$\frac{\partial W}{\partial t} + \nabla \cdot Q = E - P, \tag{2.1}$$

where W is precipitable water in the atmosphere, and

$$W = \frac{1}{g} \int_{p_s}^{p_t} q dp, \tag{2.2}$$

where g is gravity, q is the specific humidity, p_s is surface pressure, and p_t is usually considered as 300mb. Equation (2.2) represents the amount of liquid water that would result in precipitation if all the water vapor in the unit column of the atmosphere is condensed. E and P are evaporation and precipitation, respectively, and Q is the vertical integrated water vapor flux,

$$Q = \frac{1}{g} \int_{p_s}^{p_t} V q dp, \tag{2.3}$$

where V is horizontal wind vector. Precipitable water and water vapor transport are derived

from the NCEP Reanalysis II data, and $\frac{\partial W}{\partial t}$ is computed through a center finite difference scheme with a time interval of 1 day. The precipitation estimation (GPI) generated by Susskind et al. (1997) with satellite infrared observations is used as precipitation proxy. Since the observations of evaporation are not available, evaporation is estimated from the residual method (i.e. $E = P + \frac{\partial W}{\partial t} + \nabla \cdot Q$) (Yoon 1999).

2.2.1.1 Potential function and streamfunction of water vapor transport

Using Helmholtz's theorem, water vapor transport can be decomposed into the rotational (Q_R) and divergent components (Q_D) (Chen, 1985),

$$Q = Q_R + Q_D \tag{2.4}$$

Both Q_R and Q_D can be expressed in terms of their streamfunction (ψ_Q) and potential function (χ_Q), respectively,

$$Q_R = k \times \nabla \psi_Q \quad \text{and} \tag{2.5}$$

$$Q_D = \nabla \chi_Q . \tag{2.6}$$

2.2.1.2 Area averaged water vapor budget over a small region

To examine the water vapor budget over an area, each term in the water vapor budget equation can be written as

$$[P] = \int_A P dA , \tag{2.7}$$

$$[E] = \int_A E dA , \tag{2.8}$$

$$[\nabla \cdot Q] = \int_A \nabla \cdot Q dA \quad \text{and} \tag{2.9}$$

$$\left[\frac{\partial W}{\partial t}\right] = \int_A \left[\frac{\partial W}{\partial t}\right] dA. \tag{2.10}$$

Thus, the area-averaged water vapor budget can be written as

$$\left[\frac{\partial W}{\partial t}\right] + \left[\nabla \cdot Q_D\right] = [E] - [P]. \tag{2.11}$$

2.2.2 Streamfunction Budget Analysis

Typically, the global atmospheric circulation is depicted by geopotential height (Z). However, there is a disadvantage in using height fields in this study. First, this study mainly focuses on the tropical Asian region, the order of magnitude change in Z is much smaller in the tropics than in the midlatitudes. Therefore, Z is not a proper variable to portray the atmospheric circulation in the tropics. Note that the order of the magnitude of winds in midlatitude and tropics are about the same. In order to analyze the circulation pattern in Chapter 6, the streamfunction (ψ), which presents the volume rate of flow across any cross section over a designated time interval, will be applied instead of Z based on the relationship ($Z \sim \frac{\psi}{g}$).

To analyze the maintenance of the circulation, the vorticity (ζ) equation that presents the time rate change of vorticity is needed. The vorticity equation can be derived by using the approximate horizontal momentum equation. Kang and Held (1986) pointed out that the time-mean vorticity budget is noisy and difficult to interpret. Instead, they adopted the streamfunction budget analysis, which is the inverse Laplacian transform of the vorticity equation, based upon the following relationship

$$\zeta = \nabla^{-2}\psi, \tag{2.12}$$

where ψ is streamfunction.

This allows us to obtain the streamfunction budget equation from the vorticity equation (Chen and Chen, 1990),

$$\frac{\partial \zeta}{\partial t} = -V_\psi \nabla(f+\zeta) - \nabla \cdot [V_\chi (f+\zeta)] + F \tag{2.13}$$

Term1 *Term2* *Term3* *Term4*

where Term1 is the relative vorticity tendency, Term2 is the total vorticity advection, Term3 is the divergence of vorticity flux by the divergence wind, and Term4 is a combination of the tilting, vertical advection, twisting, and dissipation of vorticity. By the inverse Lapacian of the vorticity equation, the streamfunction budget equation is:

$$0 = \nabla^{-2}[-V_\psi \cdot \nabla(f+\zeta)] + \nabla^{-2} - \nabla \cdot \{[V_\chi (f+\zeta)]\} + \nabla^{-2} F \tag{2.14}$$

Term1 *Term2* *Term3*

Where Term1 is the streamfunction tendency induced by time-mean total vorticity advection through rotational flow, Term 2 is the streamfunction tendency induced by the divergence of the time-mean absolute vorticity flux with divergence flow, and Term3 is the residual term. In order to gain a better understanding of the contribution of different physical processes, Chen and Chen (1990) split the variables into their zonal and eddy components. Eq.2.14 subsequently becomes

$$0 \approx \nabla^{-2}\left(-\bar{u}_{\psi Z}\frac{\partial \bar{\zeta}_E}{\partial X}\right) + \nabla^{-2}\left(-\beta \bar{V}_{\psi E}\right) + \nabla^{-2}\left(-V_{\psi E}\frac{\partial \bar{\zeta}_Z}{\partial y}\right) + \nabla^{-2}\left(-\bar{V}_{\psi E}\cdot \nabla \bar{\zeta}_E\right)_E$$

Ψ_{A1} Ψ_{A2} Ψ_{A3} Ψ_{A4}

$$+ \nabla^{-2}\left(-f\nabla \cdot \bar{V}_{\chi E}\right) + \nabla^{-2}\left(-\bar{V}_{\chi E}\beta\right) + \nabla^{-2}\left[-\nabla \cdot \left(\bar{V}_{\chi E}\bar{\zeta} + \bar{V}_{\chi Z}\zeta_E\right)_E\right]$$

$\Psi_{\chi 1}$ $\Psi_{\chi 2}$ $\Psi_{\chi 3}$

$$+\nabla^{-2}\left[-\nabla\cdot\overline{(V'\zeta')}_E\right]+\nabla^{-2}\overline{F}_E \qquad (2.15)$$

ψ_{ts}

where ψ_{A1} is a vorticity advection term, ψ_{A2} is a advection of planetary vorticity term, $\psi_{\chi 1}$ is a stretching term, ψ_{ts} is a divergence of eddy transient vorticity flux term, and $\nabla^{-2}\overline{F}_E$ is the residual term. Through scale analysis, it was found that ψ_{A2} and $\psi_{\chi 1}$ are the largest terms in the tropics. The Eq.2.15 can be written as:

$$\psi_{A2}+\psi_{\chi 1}\approx 0 \qquad (2.16)$$

Equation 2.16 describes the approximation called the Sverdrup relation, which explains the maintenance of a stationary eddy in the tropic (Chen and Chen 1990, Chen 2004), but is not valid for the extra-tropics. Further discussion of the application of streamfunction budget in this study will be given in Chapter 6.

CHAPTER 3. THE WATER VAPOR BUDGET OVER THE SOUTHEAST ASIAN WINTER MONSOON REGION: CLIMATOLOGY

3.1 Introduction

During the winter, the weather in East Asia is dominated by a strong and steady winter monsoon, including the continent cooling and the Siberian anticyclone. In the lower troposphere, the northwesterly flows are formed along the east coast of Asia at the latitude of Japan. The flow turns southwestward near the tropic of cancer and crosses the South China Sea toward the Indonesia-Malaysian complex of islands and peninsulas. In the mean time, upward motion and large amounts rainfall occur over the "maritime continent" (Ramage 1968).

3.2 Hydrological Cycle Associated with Northern Winter Time Stationary Waves

3.2.1 Global features

The wintertime global water vapor flux is depicted with the streamfunction of water vapor flux (ψ_Q) and potential function of the water vapor flux (χ_Q) (Fig.3.1a and b). The ψ_Q shows that the strong easterly flow of the water transport is along the storm track in the north Pacific Ocean and north Atlantic Ocean. The strong westerly flow is along the tropical equator, and observations reveal that water vapor converges toward three tropical regions (the western Pacific Ocean, South America, and tropical Africa) through the local Hadley and Walker circulation (Fig.3b) (Chen 1985). To explain the maintenance of the global water vapor flux, we apply the potential function of the water vapor flux (χ_Q) and the water divergence of vapor flux (Q_D) (Chen, 1985). The largest and strongest convergence of water

vapor flux is located in the western Pacific Ocean. The convergence zone extends westward along the Intertropical Convergence Zone (ITCZ) from the tropical central Pacific through Southeast Asia to Indian Ocean. The precipitation also distributes spatially along this ITCZ.

3.2.2 Regional features

The Asian winter monsoon over Southeast Asia is characterized by the following salient features (Fig 3.2a and b):

1. The ITCZ extends westward from the Pacific into the Indian Ocean.
2. The region along the ITCZ are generally characterized by convective cloud bands and rainy weather.
3. The regions of the southern Bay of Bengal, the southern part of the South China Sea and the Philippine Sea, and a part of the western Pacific Ocean are the areas which experienced a high occurrence frequency of cold surge vortices. (Chen 2002a).

According to the third feature, our analysis included the domain associated with the major occurrence of cold surge vortices.

3.2.3 Water vapor budget analysis

To conduct a quantitative analysis of the regional hydrological cycle, area averages of individual terms in the water vapor budget equation (Eq.2.11) are computed. The computational domain includes several geographic regions: northeast Indian Ocean (A1), south of South China Sea (A2), Philippine Sea (A3), and high population areas over Southeast Asia, the Malaysian Peninsula (M), and Sumatra, Indonesia (I). The average precipitation over these areas is about $5 mm \cdot d^{-1}$ and the convergence of water vapor flux is about 1 $mm \cdot d^{-1}$ (Fig.3.2c). Since evaporation is not measured, it is evaluated by the residual method as shown in Chapter 2. As indicated by the budget analysis, precipitation is largely

maintained by evaporation supplies over 60% of water vapor to maintain precipitation (Fig.3.2c).

Cold surge vortex plays a significant role in the contribution of precipitation over Southeast Asia during the winter season. Climatologically, cold surge vortex brings over 300mm rainfall into Southeast Asia per winter season (Fig.3.2a). The rainfall over Southeast Asia is about 600mm per winter season (Fig.3.2b). Therefore, the precipitation contributed by cold surge vortices (P_{vortex}) are more than 40% of total the precipitation (P_T) over most of the area in Southeast Asia (Fig 3.3c). The ratio of P_{vortex}/P_T is particularly significant over Southeast Asia and the Philippine Sea.

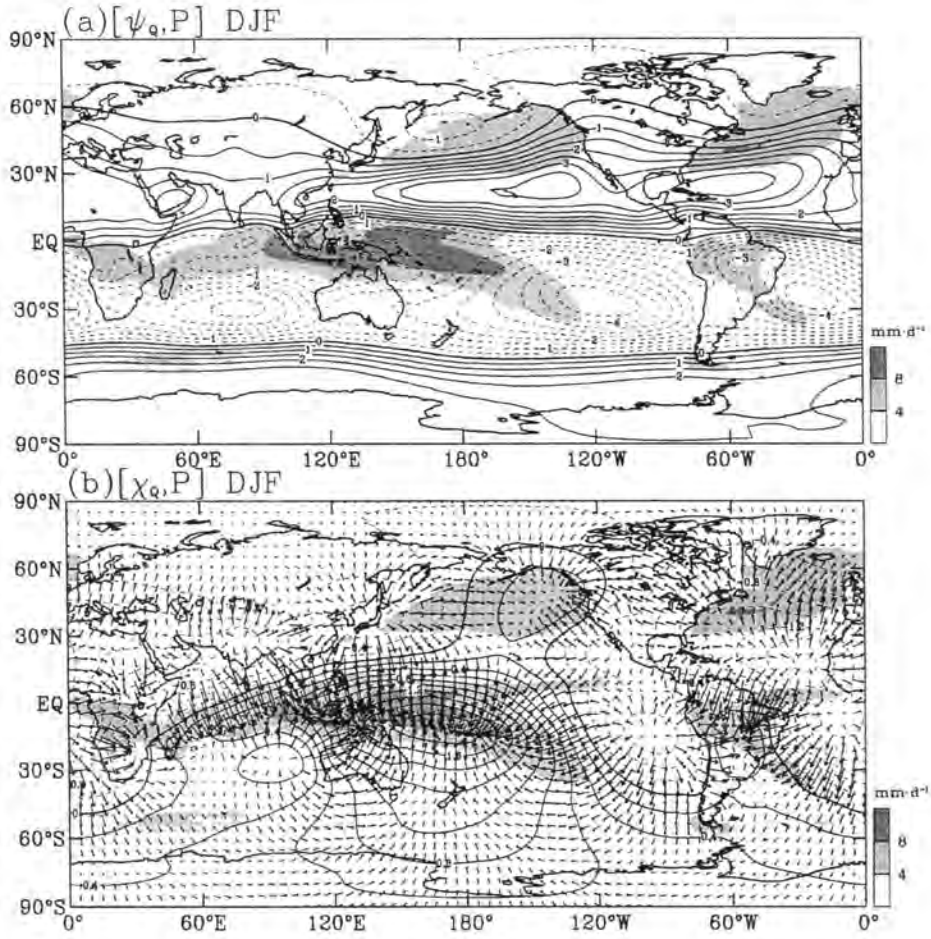

Fig.3.1. (a) Long-term winter mean for streamfunction and precipitation (ψ_Q, P). Contour interval is $5x10^6 kg \cdot s^{-1}$ for ψ_Q , and shading is the precipitation. (b) Long-term mean for the potential function, the divergent components of water vapor transport, and precipitation (χ_Q, Q_D, and P). The contour interval value is $2x10^6 kg \cdot s^{-1}$ for χ_Q

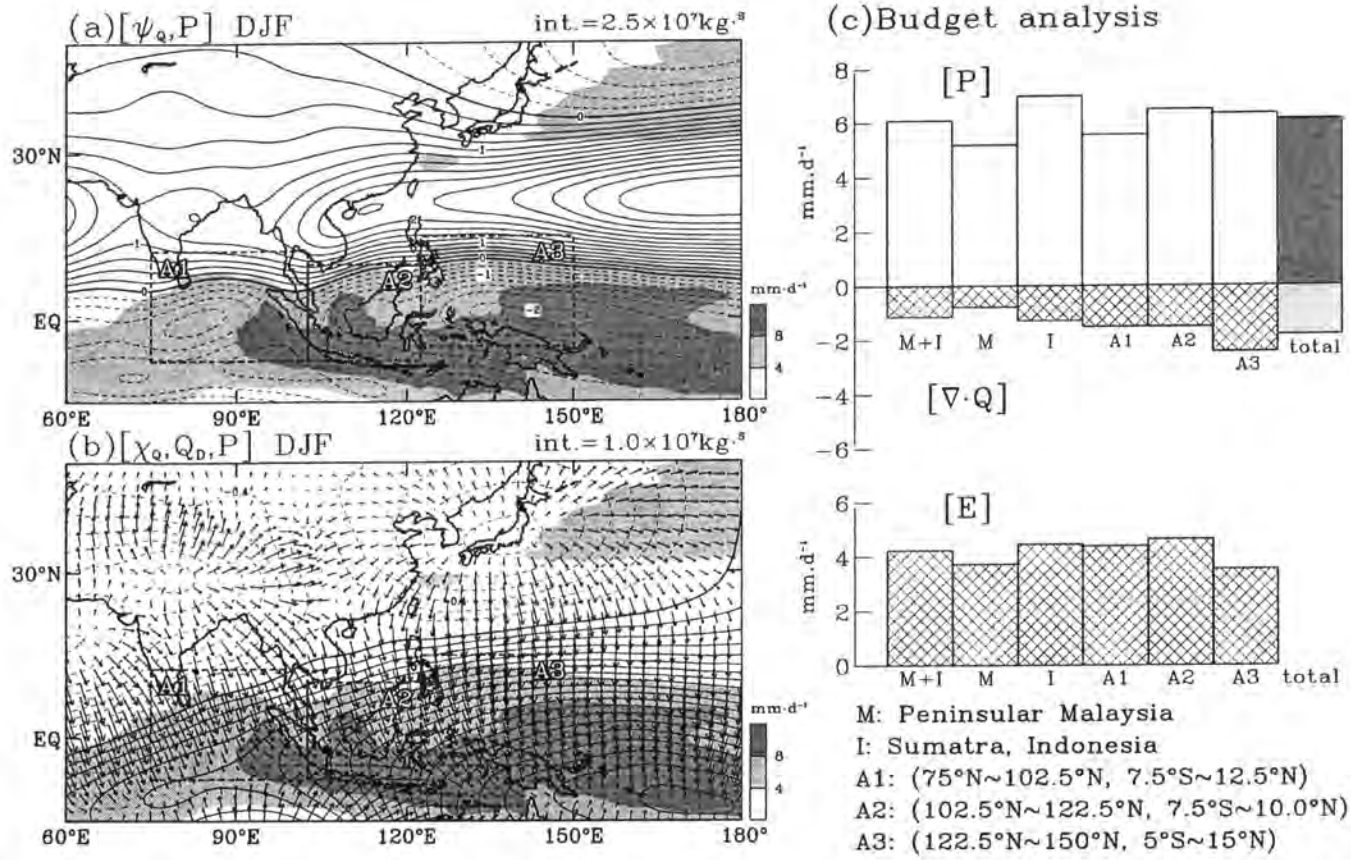

Fig.3.2 (a) and (b) are the same as Fig.3.1 (a) and (b) except for the regional domain. (c) Area averaged water vapor budget over Peninsular Malaysia, Sumatra, Indonesia, A1(75°N~102.5°N, 7.5°S~12.5°S), A2(102.5°N~122.5°N, 7.5°S~10°N), A3(122.5°N~150°N, 5°S~15°N)

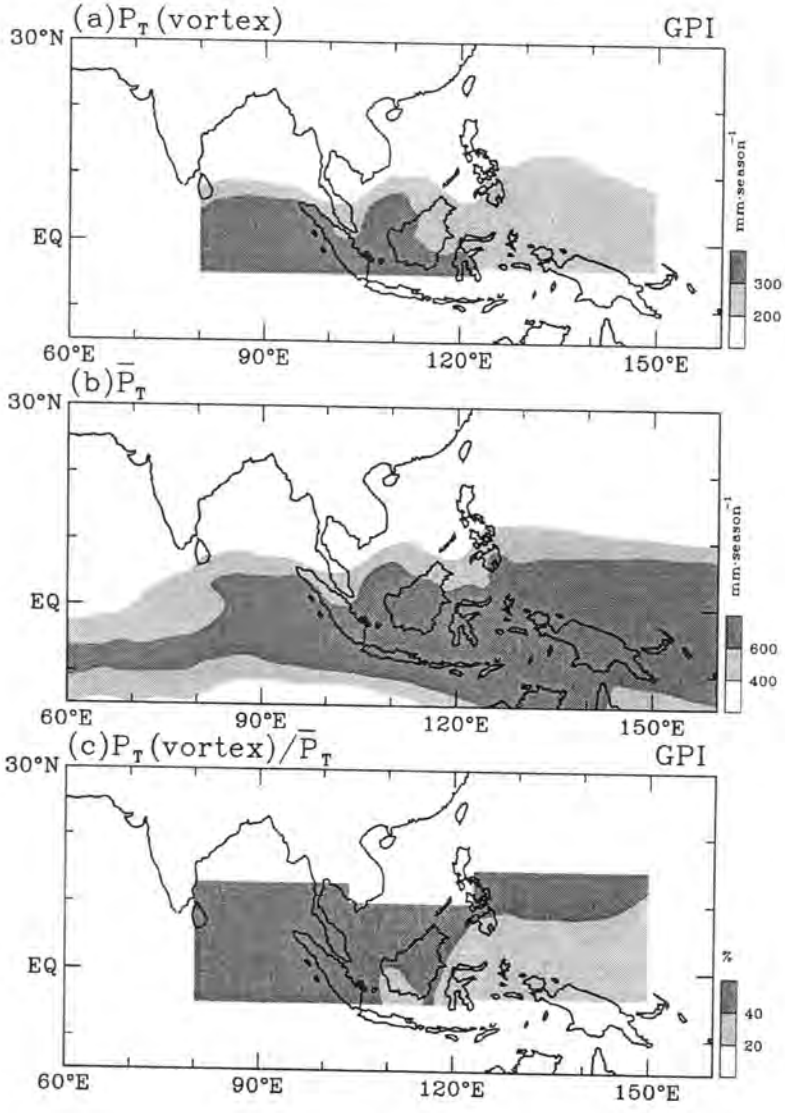

Fig.3.3. (a) Long-term mean precipitation contributed by cold surge vortices per season. (b) Long-term mean precipitation per season. (c) Percentage of the precipitation contribution by cold surge vortices.

CHAPTER 4. THE WATER VAPOR BUDGET FOR COLD SURGE VORTEX

4.1 Introduction

About 85% of the atmospheric energy source is conducted to the release of latent heat from precipitation (Chen and Chen 1994). To maintain rainfall, water vapor must be supplied through the divergence of water vapor from its source to the sink region (Chen and Chen 1994). According to Chen's (1985) analysis, the divergent component of water vapor flux is driven mainly by lower-troposphere divergent circulation. Yoon (1999) examined the water vapor budget of the Indian monsoon depression and found that the monsoon depression is primarily maintained by the convergence of water vapor flux.

Can cold surge vortex maintained by the same way through examining the water vapor budget? In this chapter, the cases that occurred in the three areas of the highest cold surge vortex occurrence (A1, A2, A3 in Fig 3.2a) will be used to explore the hydrological characteristics and the life cycle of cold surge vortex.

4.2 Hydrological Cycle Associated with a Cold Surge Vortex

Cold surge vortex can generate over half the total precipitation in Southeast Asia during winter, the major rainy season in the Southeast Asian region. It is important for us to understand how precipitation associated with cold surge vortex is maintained. A comprehensive water vapor budget analysis of three cold surge vortex cases, selected from three different high occurrence frequency areas will be used to serve this purpose.

4.2.1 A case in South China Sea: December 3 - December 8, 1993

4.2.1.1. Synoptic Analysis

A cold surge vortex was formed near Borneo, Malaysia, on Dec 3, 1993 (Fig.4.1b). When the Siberia High moved from north to south and reached the eastern seaboard of East Asia on Dec 3, 1992, a cold surge flow spiraled out over the Yellow Sea and moved all the way south to the tropical part of the South China Sea. A cold surge vortex was formed simultaneously over southwest Borneo and led to a strong tropical cumulus convection and rainfall over this region.

After the genesis stage, cold surge vortex began to move westward. The cumulus convection region of this cold surge vortex expanded further and generated more precipitation in a larger area over the South China Sea. As revealed from the contrast between Fig.4.1c and 4.1f, the convergence of water vapor flux around cold surge vortex (indicated by dashed box in Fig.4.1b) was intensified from December 3 to December 5, 1992. That is, more water vapor converged toward this cold surge vortex, to maintain the precipitation of this cold surge vortex. Cold surge vortex moved steadily westward under the southern edge of the upper-level Southeast Asian high (Fig.4.1a, 4.1d and 4.1g). The western part of this vortex crossed the Malaysian Peninsula and Sumatra, Indonesia, on December 5, 1992 (Fig.4.1e). Because of the orographic effect of the high mountains in the center of Sumatra, the vortex circulation was deformed and was able to generate another vortex. On December 6, 1992, a vortex was formed in the Indian Ocean adjacent to northwest Sumatra. This newly formed vortex moved westward to the eastern tropical Indian Ocean (Fig.4.1h).

The Siberian high in East Asia kept moving eastward during the life cycle of this cold surge vortex from December 3 to December 8, 1992. It moved across Korea and Japan and into the northwest Pacific Ocean (Fig.4.1b, 4.1e, and 4.1h). The northeasterly flow spiraling

out from the high system continued to advect cold air from the north into the South China Sea. The cold air interacted with warm air over the tropical area and interacted with cold surge vortex. This westward moving cold surge vortex in the South China Sea eventually reached the Malaysian Peninsula and then decayed and diminished there.

4.2.1.2 Water vapor budget analysis

Climatologically, evaporation over the analysis domain is about $4mm \cdot d^{-1}$ (Fig.3.2c). For the case discussed here, during the mature phase of this vortex (4~6 December), evaporation (Fig.4.1j) over this area can reach 2.5 times the climatological value (Fig.3.2c). It implies that evaporation became significant when the dry northeasterly flow moved across the warm South China Sea. Although the intensity of cold surge vortex does not reach a degree of tropical storm, the convergence of water vapor flux (Fig.4.1j) can still reach 4 times the climatological value ($2\ mm \cdot d^{-1}$) in the mature stage of cold surge vortex in the analysis domain. Consequently, both evaporation and convergence of water vapor flux bring plenty of water vapor into cold surge vortex and allow it to produce a large amount of precipitation in the mature stage. The exhaustion of moisture provided by the weaker convergence of water vapor flux and evaporation in the mature stage will deplete water vapor support from the environment and eventually lead to the dissipation of cold surge vortex.

4.2.2 A case in Philippine Sea: February 21 - February 26, 1994

4.2.2.1 Synoptic Analysis

This case was formed in the western Pacific Ocean. Unlike the previous case, the formation of this cold surge vortex was linked to an aging cold surge that had already moved out of the East Asian continent and was ahead of a newly formed cold surge over the East-Asian continent (Fig.4.1a). After its formation, this cold surge vortex continued moving

westward along the upper-level Southeast Asian trough, then across the Philippine Sea to a location between Philippines and Borneo (Figs.4.2a, b and c). During its westward propagation, the oceans moist air from the north supports cold surge vortex. On the other hand, the strong cold surge flow spiraling out of the newly formed cold surge from East Asia blocked this cold surge vortex from moving out of the Philippine Sea to enter the South China Sea. And the high system, which formed this cold surge vortex in midlatitudes, also moved westward from the East Asian continent into the North Pacific Ocean. Finally, this cold surge died in a place between Philippines and Borneo, and another cold surge vortex was induced by the new cold surge event in the South China Sea near the west coast of Borneo.

4.2.2.2 Water vapor budget analysis

Similar to the previous case, the maximum amount of rainfall also occurred during the mature stage of a cold surge vortex. As shown in Fig.4.2d, the stronger evaporation and convergence of water vapor flux are still the sources in producing/maintaining the maximum rainfall during the mature stage.

4.2.3 A case in south of Bay of Bengal: January 17-January 22, 1994

4.2.3.1 Synoptic analysis

This third case was formed in northwest Sumatra (Figs.4.2e). Like the other two cases analyzed in sections 4.2.1 and 4.2.2, this cold surge vortex had the same property of the westward propagation property (Fig.4.2e, f and g). It moved westward toward the ocean close to Sri Lanka.

Before the cold surge flow entered the Indian Ocean from the South China Sea, the northeasterly flow associated with a cold surge event may be deflected by high mountains in

the Malaysian Peninsula and Sumatra, Indonesia. This orographical interaction induces the genesis of cold surge vortex over northwestern Sumatra. After its formation, a cold surge vortex was modified by the ocean through evaporation and the convergence of water vapor flux to maintain precipitation generated by the vortex.

4.2.3.2 Water vapor budget analysis

Like the other two cases discussed earlier, the water vapor budget analysis was again preformed with this case. The maximum precipitation occurring during the mature stage was maintained by a strong convergence of water vapor flux and large evaporation (Fig.4.2h).

4.2.4 Summary

Based on our analysis, the basic characteristics of cold surge vortex can be summarized as follows.: (1) Most of cold surge vortices are induced in three areas (southern of Bay of Bengal, the southern part of South China Sea, and the Philippine Sea), but the geneses of these cold surge vortices may not occur in a uniform phase during the life cycle of cold surge events in East Asia. Most of cold surge vortices which had genesis in the Philippine Sea were induced by aging cold surge events, which had already moved away from the East Asian continent into the central Pacific Ocean. Cold surge vortices generated in the South China Sea and the eastern equatorial Indian Ocean south of Bay of Bengal usually are caused by the newly formed cold surge events in East Asia. (2) Large amounts of precipitation and water vapor of a cold surge vortex are maintained mainly by evaporation and strong convergence of water vapor flux. The latent heat released from precipitation helps develop cold surge vortex from the genesis stage into the mature phase. When the water vapor flux supply diminished, cold surge vortex steps into the dissipation phase.

4.3 Composite Analysis

Since all the cases have the same properties, a composite may be a good approach to summarize their salient features. To select the cases used for the composite analysis, the following criteria were applied:

1. A closed vortex clearly identified by a 925mb streamline chart.
2. Low-value outgoing long-wave radiation/Large-value precipitation appears with the closed vortex.
3. The identified closed vortex exhibits a clear link to the east-Asian cold air outflow/the northeast Asian cold air outbreak indicated by the 925mb streamline chart.
4. The vortex lasts more than 3 days.
5. The rainfall produced by a cold surge vortex can affect the rainfall over the Malaysian Peninsula and Sumatra.

In total, 131 cases were selected based on the criteria described above from the 1979~2001 winters. Every stage during the life cycle is composed in a consistent way through the cases and are presented in Fig.4.3. The peak of precipitation occurred during the mature stage and so did the convergence of the water vapor flux and evaporation. Comparing the climatological values over the three analysis regions (designated in Fig.1.2), the larger evaporation and stronger convergence of water vapor flux was observed when a cold surge vortex appears. Fig.4.4 shows the divergence of the water vapor flux for mature phase of the cold surge vortices. The cases mean divergence of water vapor flux is -7.8 mm/day, which is 3 to 4 times larger than the climatological value (~-2.5 $mm \cdot d^{-1}$) in the Southeast Asian region. However, the evaporation is just twice the climatological value (~4 $mm \cdot d^{-1}$) (Fig.4.3). Because precipitation should be primarily maintained by divergence of water vapor flux and

evaporation, the relationship may be written as $P \approx -\nabla \cdot Q+E$. Therefore, a stronger convergence of water vapor flux as shown in Fig.4.4 brings more water vapor into a cold surge vortex. The larger water vapor supply leads to the generation of larger rainfall over the entire life cycle of a cold surge vortex.

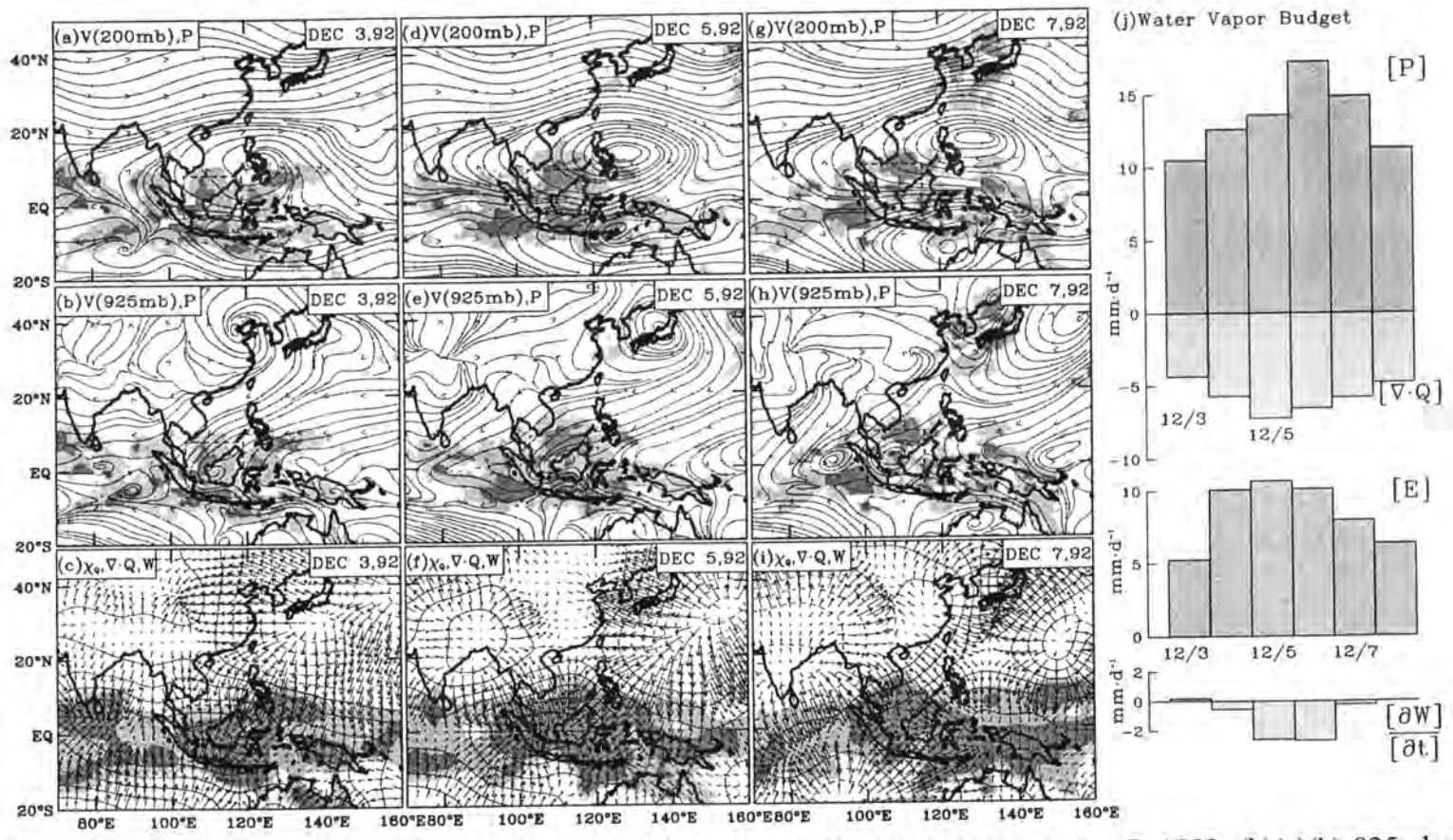

Fig.4.1 (a)(d)(g) 200mb wind field with precipitation for December 3, December 6, December 7, 1992. (b)(e)(h) 925mb wind field with precipitation for December 3, December 6, and December 7, 1993. (c)(f)(i) Potential function, the divergence components of water vapor transport, and precipitation for December 3, December 6, and December 7, 1992. (j) Area average water vapor budget for the cold surge vortex from December 3~December 8, 1992.

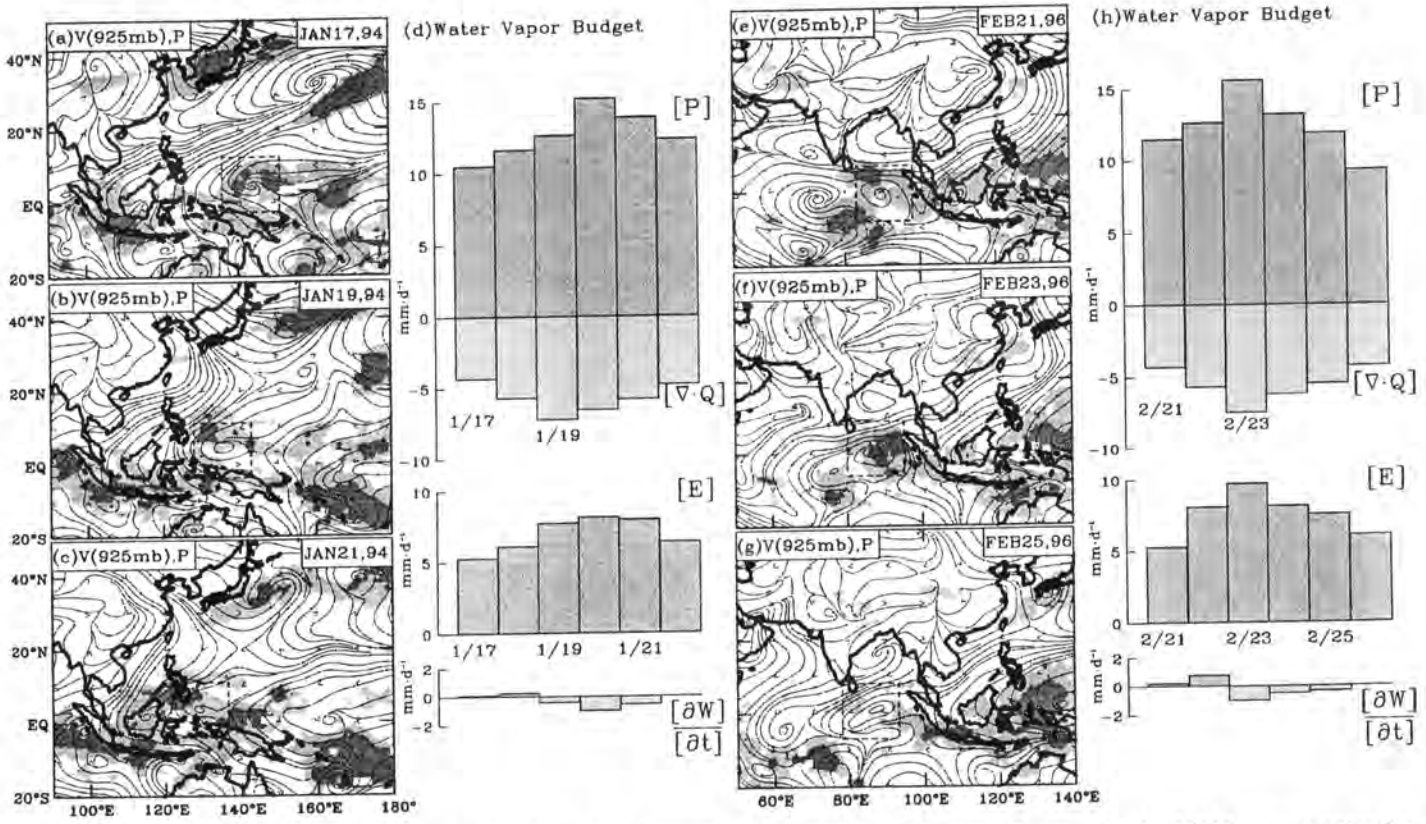

Fig.4.2 (a)(b)(c) 925mb wind field with precipitation for January 17, January 19, and January 21, 1994, respectively. (d) Area averaged water vapor budget from 17 January to 22 January 1994. (e)(f)(g) 925mb wind field with precipitation for February 21, February 23, February 25, 1996, respectively. (h) Area averaged water vapor budget from February 21 to February 26, 1996.

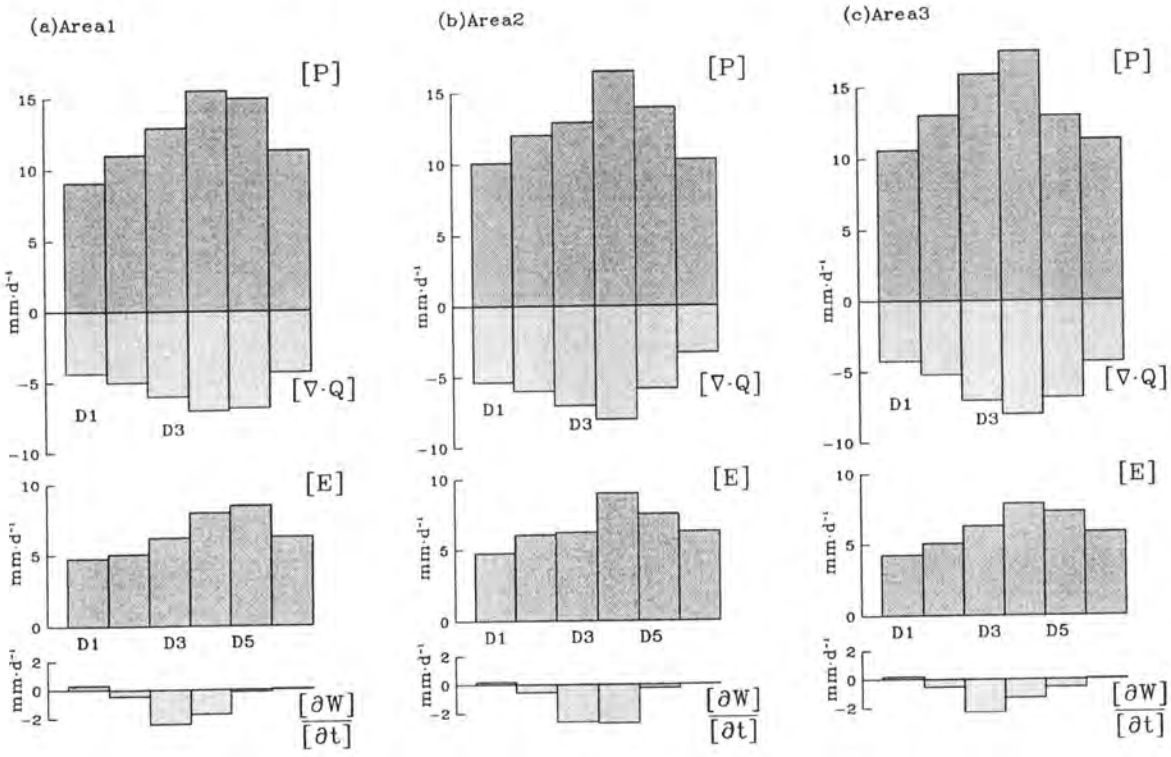

Fig.4.3 Area averaged water vapor budget composite results for (a) Area1 (75°N~102.5°N, 7.5°S~12.5°S). (b) Area2 (102.5°N~122.5°N, 7.5°S~10°N). (c) Area3 (122.5°N~150°N, 5°S~15°N)

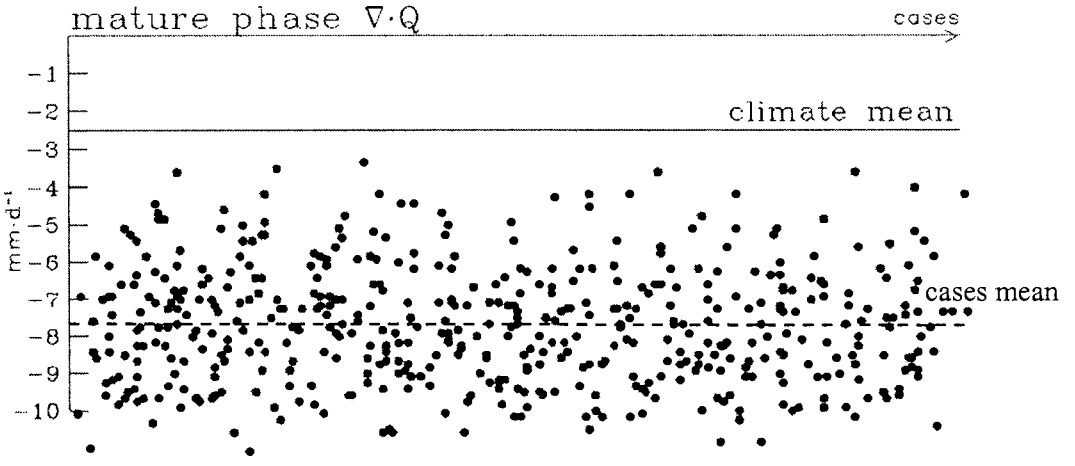

Fig.4.4 The divergence of the water vapor flux for mature phase of cold surge vortices. Soild line is the climate mean and dash line is the cases mean.

CHAPTER 5. ROLE OF COLD SURGE VORTICES IN THE INTERANNUAL VARIATION OF PRECIPITATION OVER SOUTHEAST ASIA

5.1 Introduction

5.1.1 Interannual variation of precipitation over Southeast Asia

The 1997~98 El Niño event gained considerable public awareness over Southeast Asia. For example, drought and the depletion of water resources, poorer rice yields, crop adjustment, food shortages, and forest fires. Several countries in Southeast Asia were greatly affected by its impact (Lim 2002; Glantz and Nakayama 1998)

Ropelewski and Halpert (1987) used global station precipitation data to investigate the relationship between anomalous precipitation and the ENSO event. They found that the precipitation pattern in various parts of the Asian-Australia monsoon region are coherently ENSO-related. Lau and Nath (2000) used GCM to understand the influences of the ENSO on the wintertime precipitation and circulation over the principal monsoon region of Asia and Australia. Their results showed a positive relationship between the SST index and the precipitation over Southeast Asia during winter. Southeast Asia had above-normal rainfall during the cold ENSO phase. McBride et al. (2003) used OLR data as a proxy for rainfall to check the relationship between OLR and Southern Oscillation Index (SOI); the results indicated that the maritime continent had increased rainfall during cold event.

By using the station precipitation data from the GHCN, the 24 winters of precipitation over the Malaysian Peninsula and Sumatra, Indonesia, during 1979~2002 are presented in Figs5.1a and 5.1b. and show that the interannual variation of the precipitation clearly varies

with that of the sea surface temperature over the NINO3.4 region (Figs.5.1a and 5.1b). More (less) rainfall occurs during the cold (warm) ENSO phase. The correlation coefficient between precipitation in the Malaysian Peninsula / Sumatra, Indonesia and ΔSST (NINO3.4) reaches 0.81 / 0.83. The 24 winters mean rainfall is 15mm/day (13mm/day) in the Malaysian Peninsula (Sumatra, Indinesia) .Besides 95/95 (86/87) warm winter, other warm winters are smaller than -0.8 standard deviation [σ=2mm/day and 3mm/day in the Malaysian Peninsula and Sumatra, Indinesia, respectively] in the Malaysian Peninsula (Sumatra, Indinesia). All cold winters are over 0.8σ in both places.

The anomaly of the tropical large-scale east-west circulation changes with the anomaly of the sea surface temperature in the tropical Pacific Ocean. The upward branch of the tropical Walker circulation moves eastward during the warm year, the maximum rainfall shifts eastward into the Pacific and the precipitation at the tropical western Pacific is suppressed (Holton 1992). The local weather system, either suppressed or enhanced by the change of large-scale circulation, affects the regional precipitation. To understand how the precipitation changes with the ENSO over Southeast Asia, we need to know what kind of weather system is affected by the anomalous large-scale circulation and how it affects the interannual variation of the precipitation over the Southeast Asian region.

5.1.2 Interannual variation of cold surge vortices

In Chen's (2002a) study, the occurrence frequency of cold surge vortices over the Southeast Asia has interannual variation with the sea surface temperature over the eastern Pacific Ocean. In the warm (cold) season [defined by anomalous sea surface temperatures (SST) higher (lower) than 0.5 degree over the NINO3.4 region] there were fewer (more) cold surge vortices occurring over Southeast Asia. Besides that, the interannual variation of

precipitation over the high occurrence frequency area of cold surge vortex is also coherent with the interannual variation of that of the cold surge vortex.

Chen et al. (2004) reported that the East Asian cold surge occurs more (less) frequently during warm (cold) ENSO winters. However, from Chen's (2002a) study, cold surge vortex are easier (more difficult) to form and develop when the SST over the Southeast Asian region becomes warmer (colder). Apparently, the occurrence frequency of cold surge vortices is more sensitive to western tropical pacific (WTP) SST anomalies than to the cold surge frequency reaching tropical Southeast Asia (Chen 2002a).

The most populous area in Southeast Asia is on Malaysia and Sumatra, Indonesia. By using the GHCN station data during 1979-2002 over these two areas (Fig.5.1g), we can find that the precipitation over this region has a clear interannual variation following the ΔSST (NINO 3.4) as shown in Figs5.1a and b. Malaysia and Sumatra, Indonesia, are located between the eastern tropical Indian Ocean and the South China Sea, two of the three major occurring areas of cold surge vortices. The track of cold surge vortices is not only limited to these three high occurrence frequency areas. Sometimes it moves westward, penetrates the Malaysian Peninsula or splits into two vortices near the Malaysian Peninsula and Sumatra, Indonesia. The interannual variation of the precipitation over the Malaysian Peninsular and Sumatra, Indonesia, is possibly driven by the interannual variation of the occurrence frequency of cold surge vortices that pass through or move around the area.

To verify whether cold surge vortices can affect the interannual variation of the precipitation cover Malaysia and Sumatra, Indonesia, we checked the track of cold surge vortex from 1979 to 2002. The result shows that the occurrence frequency of cold surge vortices that with its rain band covering Malaysia and Sumatra, Indonesia during 1979 to

2002 has the coherent interannual variation with ΔSST (NINO3.4) (Fig.5.1b and 5.1e). More cold surge vortices pass through Malaysia and Sumatra, Indonesia can contribute more precipitation in this area, while fewer cold surge vortices bring less precipitation into this area. Hence, the interannual variation of the precipitation can also be explained by the occurrence frequency of cold surge vortices that pass through Malaysia and Sumatra, Indonesia.

In Chapter 4, we showed the large convergence of water vapor flux is an important feature of cold surge vortex, which helps maintain the precipitation brought by cold surge vortex. Is this character also the key that makes the interannual occurrence frequency of cold surge vortices capable of dominanting the interannual variation of the precipitation in Southeast Asia? To answer this question, the water vapor budgets of cold surge vortices over the 24 winters (1979-2002) are performed.

5.2 Water vapor budget analysis

To perform the water vapor budget analysis, the three high cold occurrence area of the surge vortices, south of Bay of Bengal, south of the South China Sea, and the Philippines Sea (Chen 2002a) are included for the water vapor budget analysis. The Malaysian Peninsula and Sumatra, Indonesia, where the interannual variation of precipitation responds to the occurrence frequency of cold surge vortices as well as ENSO phase (Fig.5.1a and b), are considered in the analysis for comparison. The detail area map is shown in Fig.5.2c.

Since the GPI is available only during 1979~1980 and 1988~1997, the gap over the 24 winters (1979-2002) is filled by the precipitation from the NCEP reanalysis II with a comparison of OLR. Arkin and Ardanuy (1989) suggested that ΔOLR(=235Wm^{-2}-OLR) is a

reasonable rainfall proxy over the active convection region in the Tropic. Chen (2002a) used this proxy to estimate the percentage of the rainfall contributed by cold surge vortices and suggested that the result is similar to that estimated by the GPI data. Chen's (2002a) results also indicate that the contribution of cold surge vortex to total seasonal rainfall is particularly significant over Southeast Asia and the Philippine Sea.

From our water vapor budget analyses of 24 winters over the regions defined in Fig.5.2c, the precipitation, divergence of water vapor flux, and evaporation all responded to the ENSO phases (Fig.5.2a). The precipitation over Southeast Asia increases (decreases) during the cold (warm) ENSO phase. The convergence (divergence) of water vapor flux associated with the evaporation increases (decreases) during the cold (warm) ENSO phase. Interannually, the tropical Pacific SSTs exhibit an east-west seesaw in concert with the ENSO cycle (Rasmusson and Carpenter 1982). The warm/cold SST anomalies in the western tropical Pacific (WTP) respond to the cold/warm ENSO phase. During the cold (warm) ENSO event, the SST in the WTP increases (decreases) and induces more (less) evaporation. The water vapor increases (decreases) when the evaporation from the ocean surface increases (decreases). The high moisture is favorable to the generation of cold surge vortex and in turn produces more precipitation.

To understand how much precipitation (P), divergence of water vapor flux ($\nabla \cdot Q$), and evaporation (E) are contributed from cold surge vortices, the ratios of $P_{vortex}/P_{T,}$ $\nabla \cdot Q_{vortex}/\nabla \cdot Q_T$ and E_{vortex}/E_T are estimated, where the subscript "vortex" means the contribution from vortex and "T" means the total amount. As shown in Fig.5.2b, these three ratios reveal that cold surge vortices contribute, in average, more than half the precipitation, convergence of the water vapor flux, and evaporation over Southeast Asia during winter. This

contribution undergoes a pronounced interannunal variation with the ENSO phase. Cold surge vortices bring about 80% of winter monsoon rainfall, divergence of the water vapor flux, and evaporation during cold ENSO winters, but only about 40% during warm ENSO winters. The correlation coefficient between precipitation contribution by cold surge vortices and ΔSST (NINO3.4) reaches 0.82. The correlation coefficient between divergence of water vapor flux (evaporation) contributed by cold surge vortices and ΔSST (NINO3.4) reaches 0.84 (0.86). The 24 winters mean for precipitation, water vapor flux and evaporation are 570 mm/season, -250mm/season and 320mm/season, respectively. Except for the 98/99, and 99/00 winters, all other cold winters are over 0.8σ (σ=150mm/season, σ=80mm/season, and σ=90mm/season for precipitation, divergence of water vapor flux and evaporation, respectively, while the warm winters are smaller than -0.8σ (86/87, 91/92, 97/98, 02/03).

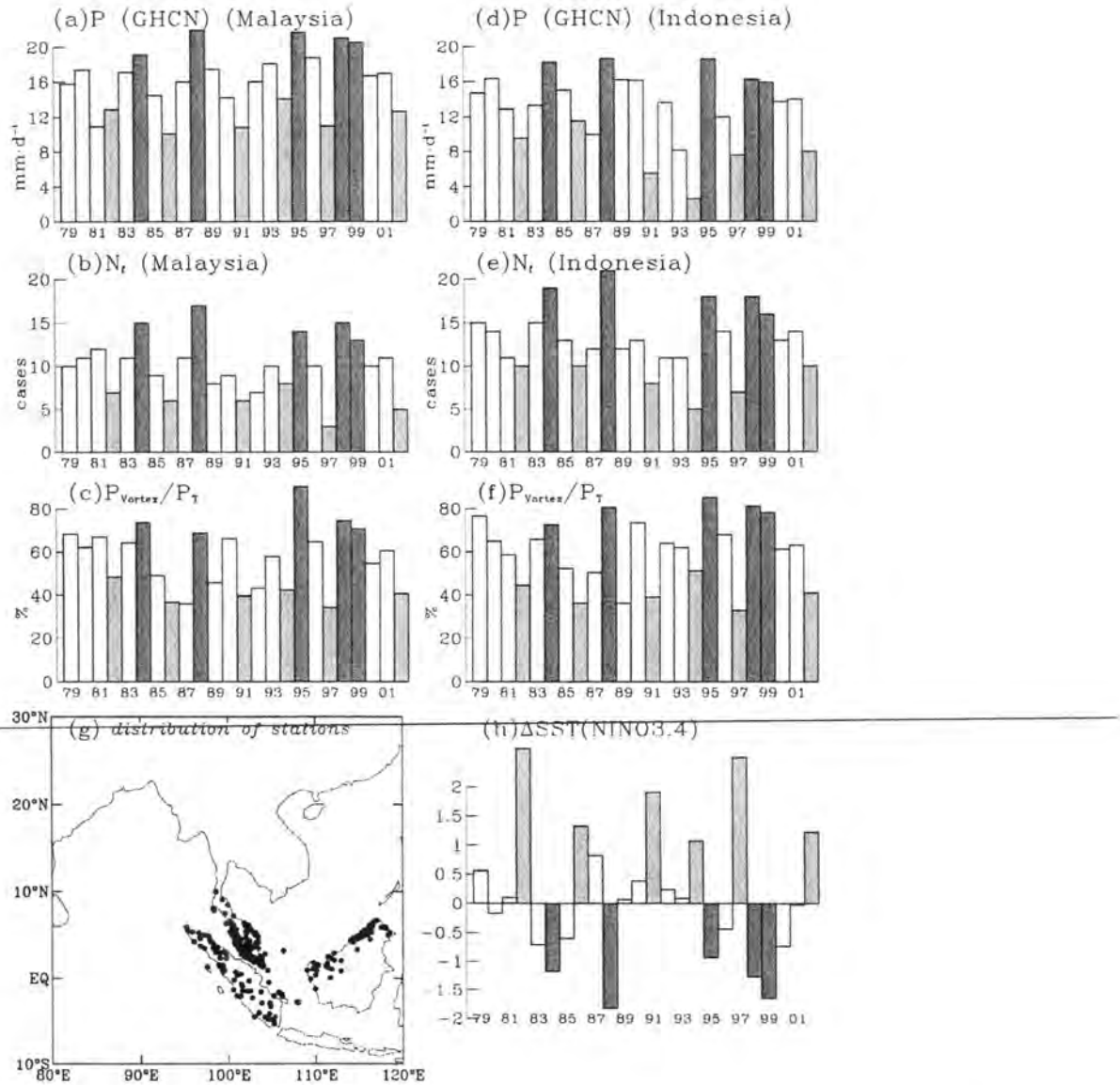

Fig.5.1. (a) and (d) are precipitation from GHCN for Malaysia and Indonesia from 79~02. (b) and (e) are cold surge vortices occurrence frequency for Malaysia and Indonesia. (c) and (f) are precipitation contributed by cold surge vortices for Malaysia and Indonesia. (g) Distribution of the GHCN station used in the study. (h) Anomaly sea surface temperature over NINO3.4 region. Histograms of cold and warm ENSO winters are indicated by dark and gray color, respectively.

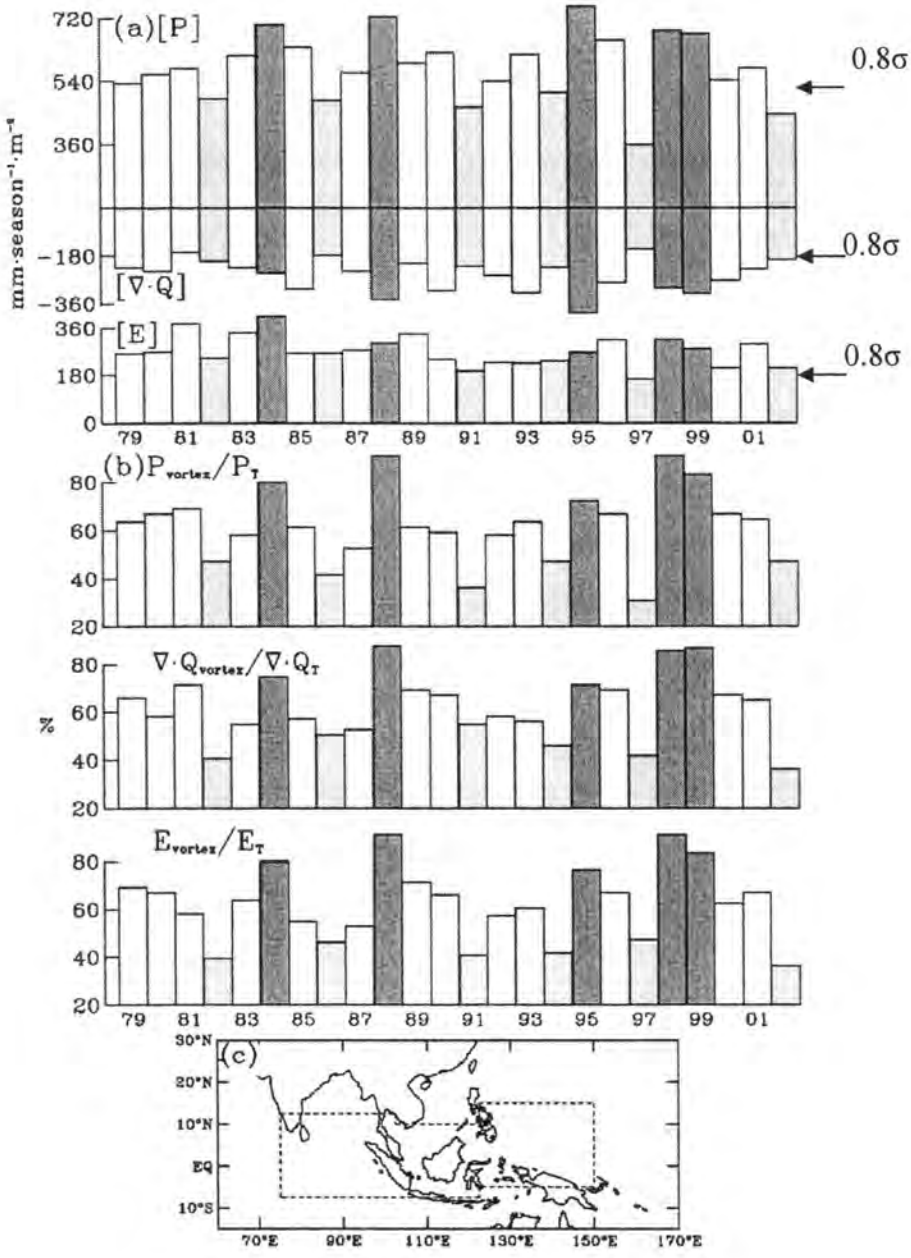

Fig.5.2 (a) Histogram of rainfall (P), divergence of water vapor flux ($\nabla \cdot Q$), and evaporation (E) of every winter average over the region defined in (c). (b) total (P_T, $\nabla \cdot Q_T$, E_T) contribution from cold surge vortices ((P_{vortex}, $\nabla \cdot Q_{vortex}$, E_{vortex}), and ratio P_{vortex}/P_T, $\nabla \cdot Q_{vortex}/\nabla \cdot Q_T$, E_{vortex}/E_T. Histograms of cold and warm ENSO winters are denoted by dark and gray color, respectively. The encircled regions in (c) are designated for water vapor budget analysis.

CHAPTER 6. ROLE OF COLD SURGE VORTICES IN LARGE SCALE CIRCULATION

6.1 Introduction

East-Southeast Asia is covered by the winter monsoon, one of the most energetic circulations and active convective systems of the atmosphere (Lau and Chang 1987). During the transition between the Asian summer and winter monsoon, the summertime upper-level Tibetan anticyclone gradually disappears. Meanwhile, an upper troposphere anti-cyclone, known as the Southeast Asian high, is gradually formed in the north Philippine Sea.

By compiling all available observation data, Krishnamirti et al. (1973) was the first to portray the winter circulation. They showed that three active convection areas emerge from tropical continents and maintain three upward branches of the tropical east-west circulation. These tropical convection centers are located over tropical South American, equatorial Africa, and around the maritime continent. Like the summer (June, July, Aug) atmospheric circulation (Krishnamirti, 1971), the divergent center is in phase with the vorticity center in the tropical region. In order to obtain a proper simulation of the monsoon high, Holton and Colton (1972) used the winter observation data provided by Krishnamirti and incorporated the sub-grid scale dissipation term in their diagnostic model.

Gill (1980) used a simple shallow water analytic model to elucidate some basic features of the response of the tropical atmosphere to diabatic heating. He pointed out that the rising motion, due to heating, causes vortex stretching and, hence, acquisition cyclonic vorticity. There is a considerable east-west asymmetry that can be illustrated by solution of the heating concentrated in an area of finite extent. The circulation in response to this heating

is called the Walker circulation. In Gill's solution, the heat source is in a quarter phase shift with the streamfunction field. However, this quarter phase shifted relationship contradicted Krishnamirti's (1971) depiction of the tropical circulation.

The spatial quadrature relationship between the upper-level streamfunction and velocity potential during the summer season (Hoskins et al. 1989; Schubert et al. 1990) exists in the post-FGGE data analyzed by the European Centre for Mid-Range Weather Forecast (ECMWF). Hoskins (1996) presented the vertical integrated diabatic heating fields and from his results showed that the east-west circulation of the Asian monsoon is maintained by North African cooling and the western Pacific-Asian monsoon heating. The Tibetan anticyclone, which is an important upper-level element of the Asian monsoon, is juxtaposed with the ascending motion to its east and descending motion to its west. The spatial quadrature relationship between this monsoon high and the east-west circulation meets the requirement of the Sverdrup balance (Eq.2.16).

Since the disagreement of the maintenance of the monsoon anticyclone between the prior and post FGGE data, Chen (2002b) performed the streamfunction budget analysis with the NCEP-NCAR reanalysis data to explore the maintenance of monsoon circulation. He demonstrated that the summertime East Asian monsoon anticyclone is maintained by the east-west differential heating through the Sverdrup balance. By using the same approach, Chen (2004) showed that the Southeast Asian high is also maintained by the east-west differential heating through the Sverdrup relationship. The quarter phase shifted relationship exists between the anticyclone and east-west circulation in the tropical region during the winter is different from the in-phase relationship between the convergence (divergence) center and the low (high) pressure center as depicted by Streten and Zillman (1984).

It is shown in the early chapters that cold surge vortices contribute a half of the Southeast Asian winter monsoon precipitation. These vortices that may be the forcing of the transient component of the Southeast Asian circulation was excluded in Chen's (2004) maintenance dynamics. It is the purpose of this chapter to explore the role played by those transients eddy forcing induced by cold surge vortices in maintaining the Southeast Asian high.

6.2 Maintenance of northern wintertime stationary wave

In the winter monsoon region over East and Southeast Asia, three distinct features of monsoon circulation (Chen 2004) are revealed from Fig.6.1:

- The east-west circulation coupled with the Southeast Asian high, where the upward branch is located over the central tropical Pacific Ocean, and the downward branch is situated west of the Indian Ocean (Fig 6.1b).
- A monsoon low under the Southeast Asian high (Fig.6.1c) indicating a vertical phase reversal of the tropical circulation in the monsoon system is revealed from the cross section of the eddy of streamfunction (ψ_E) (10°~15°N) (Fig.6.1b).
- The Southeast Asian high (low) and the upper-(lower)-level divergent circulations are spatially in quadrature.

The basic features of the winter stationary waves were observed to formulate the basic dynamic of the stationary wave, the simplification of the vorticity equation by a scale analysis (e.g., Charney 1948, Burger 1958) is often applied. To simplify the streamfunction budget equation, the development of these criteria is based upon the following principles: 1) the spatial structure of the streamfunction tendency induced by a dynamic process exhibits a

spatially systematic relationship with streamfunction and 2) the variance explained by this streamfunction tendency should be significant when compared with those caused by other dynamic processes (Chen and Weng 1999). Any term in the complete streamfunction budget equation with its variance satisfies one of the two criteria is neglected: $Var(\psi_{An})/Var(\psi_A)\leq 15\%$ or $Var(\psi_{\chi n})/Var(\psi_\chi)\leq 15\%$

Based on these two principles, the nonlinear (ψ_{A3}, $\psi_{\chi 2}$ and $\psi_{\chi 3}$) and transient terms (ψ_{ts}) in the complete streamfunction budget equation (Eq.2.15) are negligible (Chen 2004). Hence, the streamfunction budget for the winter climatology in the middle-high latitude can be summarized as

$$\psi_{A1}(200mb)+\psi_{A2}(200mb)+\psi_{\chi 1}(200mb)\cong 0 \text{ and} \tag{6.1}$$

$$\psi_{A2}(850mb)+\psi_{\chi 1}(850mb)\cong 0 \tag{6.2}$$

Since the zonal wind speed is much smaller in the tropics as compared to the mid-latitudes, the vorticity advection term (ψ_{A1}) can be neglected in (Eq.6.1) for the tropics (Chen 2004). Therefore, the streamfunction budget can be summarized as the Sverdrup balance in the tropics (Chen 2004),

$$\psi_{A2}(200mb)+\psi_{\chi 1}(200mb)\cong 0 \tag{6.3}$$

$$\psi_{A2}(850mb)+\psi_{\chi 1}(850mb)\cong 0 \tag{6.4}$$

As revealed from the streamfunction budget over the Southeast Asia (Fig.6.2), one can determine that

- The ψ(200mb) are spatial in quadrature with their corresponding ψ_{A2} (200mb), while ψ(850mb) are in quadrature with the ψ_{A2}(850mb).

- An opposite polarity exists between $\psi_{\chi 1}$(200mb) and ψ_{A2}(200mb) as well as between $\psi_{\chi 1}$(850mb) and ψ_{A2}(850mb).
- The opposite polarities exist in the $\psi_{\chi 1}$ and χ.

The east-west circulation with the upward motion is located in the tropical central Pacific and the downward branch is located in the western Indian Ocean is the major dynamical element, among various dynamic processes of the streamfunction budget, in maintaining the Southeast Asian high (Chen 2004).

6.3 Composite Analysis

To understand the role played by cold surge vortex in the large-scale circulation, we need to examine the difference between cold surge vortices cases and non-cold surge vortices cases by applying the composite analysis. To process the composite analysis, the days while cold surge vortices existed over Southeast Asia are selected and averaged. To portray the circulation, the ψ and χ, which are the inverse of the Laplacian on vorticity and divergence fields, are applied here. The criteria used in section 4.3 are applied here to select those cases.

6.3.1 Discussion

Following the criteria, about 80% of the days of the 23 winters during 1979-2001 are selected. In order to emphasize the impact from cold surge vortex, we show the difference between the total cases and noncases composite. The anomalous circulation between the cases and noncases composites (Fig.6.3) shows that the upper-level East Asia midlatitude jet speeds up associate with the following features:

1. The upper-level Southeast Asian High is intensified (Fig.6.3a), and the low level

monsoon low is correspondingly deepen (Fig.6.3c).

2. A vertical phase reversal of the tropical anomalous circulation (10°~15°N) (Fig.6.3b) emerge from the contrast between $\Delta\psi$(200mb) (Fig.6.3a) and $\Delta\psi$(850mb) (Fig.6.3c).
3. The spatially quadrature relationship between the monsoon high (low) and tropical divergent circulation is revealed from the $\Delta\psi$ and $\Delta\chi$ fields at 200 and 850mb.

Actually, this quadratic relationship can be demonstrated as well by superimposing the east west circulation (u_D, $-\omega$)(10°~15°N) with the $\Delta\psi$ cross-section of (10°~15°N) (Fig.6.3b). The updraft of the east-west circulation appears in the east side of the Southeast Asian high, while the downdraft branch is formed in the west side of this anticyclone. What is the dynamic mechanism in maintaining this spatially quadratic featured? This question will be answered by using the streamfunction budget analyses in the anomalous circulation.

6.3.2 Maintenance of the anomalous circulation

Following the criteria in section 6.2.1, the simplified streamfunction budget analysis in the anomalous circulation is shown in Fig.6.4. According to the unbalanced pattern between ψ_{A2} and $\psi_{\chi 1}$, the result shows that, in the tropics (within the box in Fig.6.4), the Sverdrup balance (Eqs.6.3 and 6.4) cannot to fully explain the anomalous circulation over Southeast Asia. To compensate, the anomalous divergence of transient vorticity flux ($\Delta\psi_{ts}$) needs to be taken into account. To quantitatively express the balancing situation in the budget analysis, we calculate the ratio between these terms. The percentage of Var($\Delta\psi_{\chi 1}$)/Var($\Delta\psi_{A2}$) is less than 75% at both 200mb and 850mb in Southeast Asia, which does not satisty the Sverdrup balance. After adding $\Delta\psi_{ts}$, the Var($\Delta\psi_{\chi 1}+\Delta\psi_{ts}$)/Var($\Delta\psi_{A2}$) exceeds 90% at both levels,

indicating that the approximated dynamic process should be:

$$\Delta\psi_{A2}(200\text{mb})+\Delta\psi_{\chi 1}(200\text{mb})+\Delta\psi_{ts}(200\text{mb})\approx 0 \quad (6.5)$$

$$\Delta\psi_{A2}(850\text{mb})+\Delta\psi_{\chi 1}(850\text{mb})+\Delta\psi_{ts}(850\text{mb})\approx 0 \quad (6.6)$$

The quantity of $\Delta\psi_{ts}$ at 200mb for the case—noncase composite is present in Fig.6.4d. The transient vorticity fluxes systematically reinforce the vortex stretching effect and help maintain the anomalous upper-troposphere rotational flow during cold surge vortices composite. The $\Delta\psi_{ts}$ (Fig.6.4d) shows a regional significance and is a non-negligible component in maintaining the anomalous circulation associated with cold surge vortex over Southeast Asia.

The transient term has traditionally been assumed to be relatively small when the mean vorticity budget was examined (Hurrell 1995). However, Hurrell (1995) demonstrated that the transient vorticity flux is capable of maintaining the upper-troposphere rotational flow anomalies during the North Atlantic Oscillation (NAO) phase. In this study, divergence of transient vorticity flux (ψ_{ts}) is negligible [$\text{Var}(\psi_{ts})/\text{Var}(\psi_{\chi})<5\%$] when dealing with the long term winter mean, which the Sverdrup balance (Eqs.6.3 and 6.4) dominates the dynamics in the tropical circulation. But when we explain the anomalous circulation, the anomalous divergence of transient vorticity flux ($\Delta\psi_{ts}$) is larger over Southeast Asia due to [$\text{Var}(\Delta\psi_{ts})/\text{Var}(\Delta\psi_{\chi})>15\%$]. In other words, we should add the $\Delta\psi_{ts}$ into the Sverdrup balance (Eqs. 6.5 and 6.6) to explain the anomalous circulation caused by cold surge vortex in Southeast Asia.

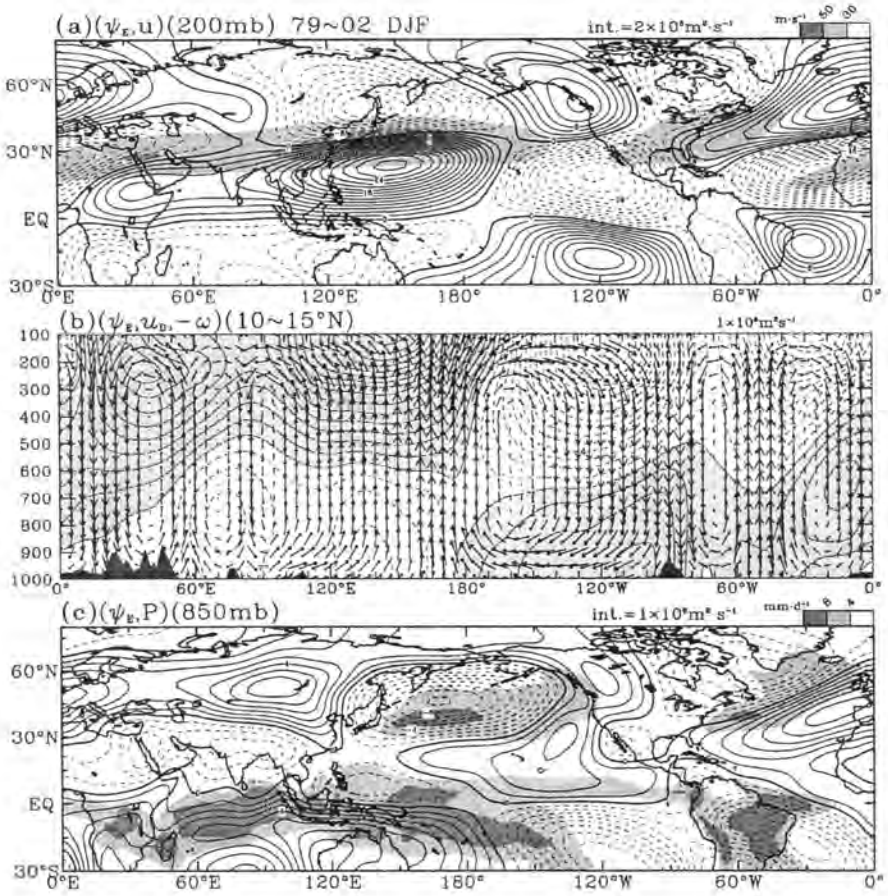

Fig.6.1. Long-term mean wintertime streamfunction for (a) 200mb, shading is the zonal wind speed (c) 850mb, shading is the precipitation, (b) vertical cross section across tropical (10^{o}N~15^{o}N), contour is the eddy component of the streamfunction. The contour value is $2\times10^{6}m^{2}s^{-1}$ for (a) and $1\times10^{6}m^{2}s^{-1}$ for (b) and (c) [adopted from Chen (2004)].

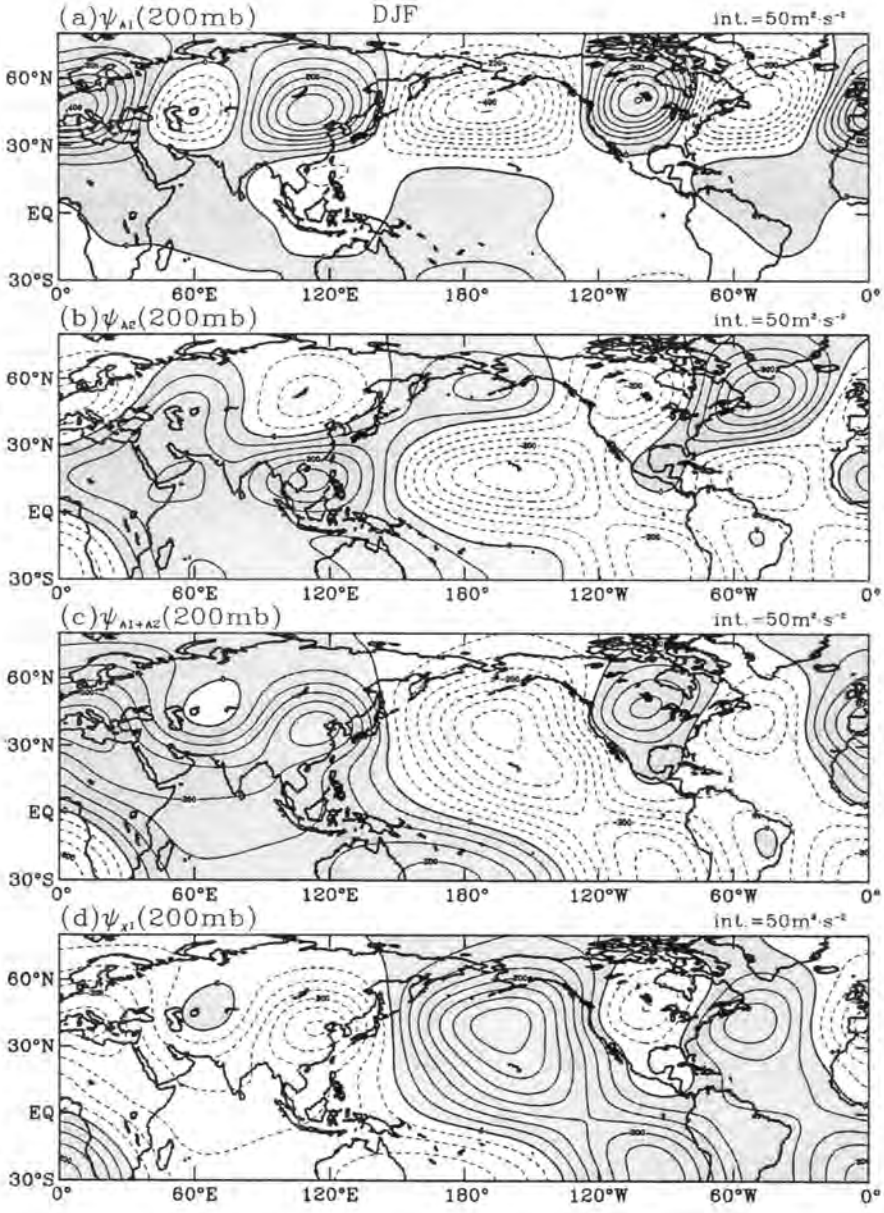

Fig.6.2. Long-term mean wintertime streamfunction budget for 200mb (a) ψ_{A1} (b) ψ_{A2} (c) ψ_{A1+A2} (d) $\psi_{\chi 1}$. The contour interval for those charts are $50m^2s^{-2}$.

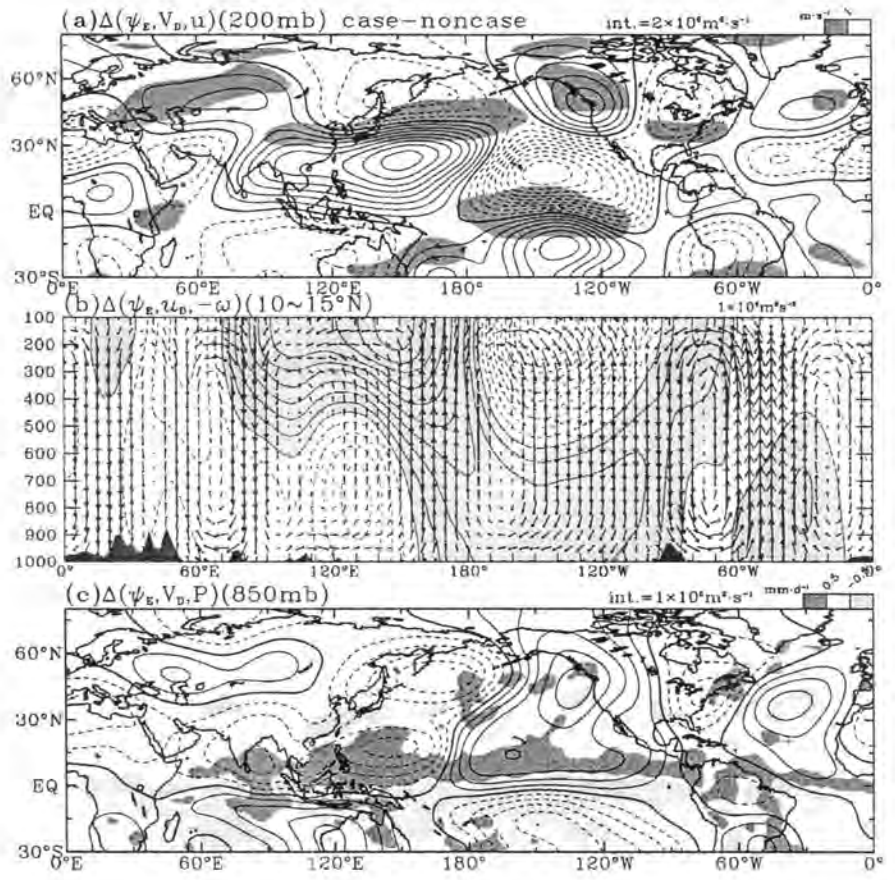

Fig.6.3 Departures of composite eddy (ψ_E) during vortex cases from noncase at (a) 200mb, superimposed with the zonal wind speed (c) 850mb, shading is the precipitation, (b) vertical cross section across tropical (10^oN~15^oN), contour is the departure of the streamfunction. The contour value is $2\times10^5 m^2 s^{-1}$ for (a) and $1\times10^5 m^2 s^{-1}$ for (b) and (c).

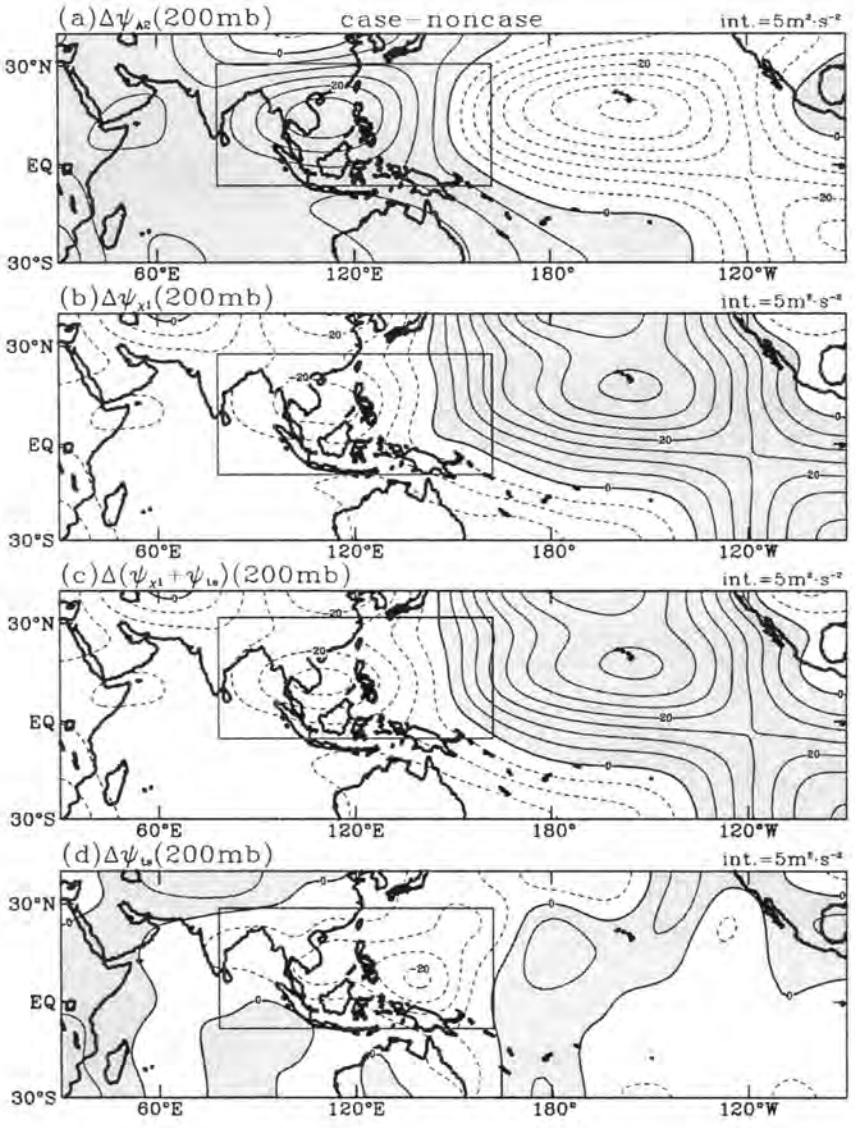

Fig.6.4 Streamfunction budget analysis in the anomalous circulation at 200mb (a) $\Delta\psi_{A2}$ (b) $\Delta\psi_{\chi l}$ (c) $\Delta\psi_{\chi l}+\Delta\psi_{ts}$ (d) $\Delta\psi_{ts}$. The contour interval for those charts are $5m^2s^{-2}$. The encircle box is the Southeast Asian region, where the Var($\Delta\psi_{ts}$)/ Var($\Delta\psi_{A2}$)>15%.

CHAPTER 7. CONCLUSIONS

The hydrological cycle associated with the winter cold surge vortices is examined in this study through using the NCEP II reanalysis, GHCN, GPI and OLR data. First, winter is the major rainy season in Southeast Asia. Second, cold surge vortices can contribute more than half of the annual precipitation during the winter. Third, the water vapor budget analysis shows that the interannual variation of the occurrence frequency of cold surge vortices is proportional to that of the interannual variation of precipitation anomalies in Southeast Asia. Finally, cold surge vortex is associated with the considerable transient activity over Southeast Asia that becomes an important driving force to maintain the anomalous circulation over Southeast Asia.

The center of the water vapor flux divergence moves to the tropical Western Pacific Ocean from the coast of East Asia during winter. The amount of precipitation increases in the Southeast Asian countries due to the generation of cold surge vortex induced by the interaction of cold surge and the tropical warm air. During this season, the monsoon trough, monsoon disturbances, and the circulation interaction between the mid-latitude and tropics become the major research topics in the region. The major findings in this study can be summarized as follows.

7.1 Cold surge vortices

The cold surge coming from Siberia becomes the monsoon northeasterly in Southeast Asia. The cold surge usually forms a cold surge vortex. Around the tropical area, cold surge vortex is one of the major precipitation types over Southeast Asia during winter.

The water vapor analysis shows that cold surge vortices have a strong convergence of the water vapor flux, which stores more precipitable water in the cold surge vortex. This

makes cold surge vortex be capable of bring huge amounts of precipitation to Southeast Asia.

7.2 Interannual variation

The interannual variation of the precipitation over Southeast Asia has a clear distinction depending on two interannual variations [warm/cold defined by the ΔSST (NINO3.4) and wet/dry defined by the precipitation amount].

Cold surge vortices also show a clear interannual variation following the warm and cold winters. Cold surge vortices occur more (less) during cold (warm) years. By using the water vapor budget analysis, the divergence of the water vapor flux contributed by cold surge vortices dominates the regional divergence of water vapor flux over Southeast Asia. Since the water vapor flux maintains the water vapor content, the low (high) water vapor flux convergence makes less water vapor content in the region during warm (cold) ENSO events and in turn leads to fewer (more) precipitation amounts falling over Southeast Asia.

7.3 The role played by the cold surge vortices in large scale circulation

The Sverdrup balance is adequate to explain the tropical circulation during winter. The differential east-west vertical motion can maintain the Southeast Asian high through the stretching and advection of planetary vorticity (Chen 2004). The anomalous circulation caused by cold surge vortex can intensify the Southeast Asian high. However, the maintenance of the anomalous circulation caused by cold surge vortex cannot be fully explained by the Sverdrup balance in Southeast Asia. The anomalous divergence of transient vorticity flux ($\Delta\psi_{ts}$), which is contributed by the cold surge vortex, must be considered in this area when we are dealing with the maintenance of the anomalous circulation caused by cold surge vortex, particularly over Southeast Asia.

REFERENCES

Arkin, P. A., and P. E. Ardanuy, 1989: Estimating climate-scale precipitation from space: A review. *J. of Clim.*, **2**, 1229-1238

Berlate, H. P., 1927: East monsoon forecasting in Java. Berhandelingen No. 20, Knoinklijk Magnetisch en Meteorologisch Observatorium te Batavia, Batavia, Indonesia.

Bjerknes, J., 1969: Atmospheric Teleconnections from the Equatorial Pacific: *Mon. Wea. Rev.*, **97**, 163-172.

Braak, C., 1921-1929: Het Climaat van Nederlandsch Indie. *Magnet. Meteorol. Observ. Batavia, Verhand.* **8**.

Brakk, C., 1919: Atmospheric variations of short and long duration in the Malay Archipelage. Verhandelingen No. 5, Koninklijk Magnetischen Meteorologisch Observatorium te Batavia, Batavia, Indonesia.

Burger, A., 1958: Scale consideration of planetary motions of the atmosphere. *Tellus*, **10**, 195-205.

Chang, C.-P., J. E. Erickson and K. M. Lau, 1979: Northeasterly Cold Surges and Neat-Equatorial Disturbances over the Winter MONEX area During December 1974. Part I: Synoptic Aspects: *Mon. Wea. Rev.*, **107**, 812-829.

Chang, C.-P., and K. M. W. Lau, 1980: Northeasterly Cold Surges and Neat-Equatorial Disturbances over the Winter MONEX area During December 1974. Part II: Planetary-Scale Aspects: *Mon. Wea. Rev.*, **108**, 298-312.

Charney, J. G., 1948: On the scale of atmospheric motion. *Geofys. Publ.*, **17**.

Cheang, B. K., 1977: Synoptic feature and structure of some equatorial vortices over the South China Sea in the Malaysian region during the winter monsoon of the December

1973. *Pure Appl. Geophy.* **115**, 1303-1333.

Cheang, B. K. 1987: Short- and Long-Range Monsoon Prediction in Southeast Asia. *Monsoons*, ed. By J. S. Fein and P. L. Stephens, John Wiley & Sons (ISBN 0-471-87416-7), 579-606.

Chen, T.-C., 1985: Global Water Vapor Flux and Maintenance during FGGE: *Mon. Wea. Rev.*, **113**, 1801-1819.

Chen, T.-C. and J.-M. Chen, 1990: On the Maintenance of Stationary Eddies in Terms of the Streamfunction Bueget Analysis: *J. of Atmos. Sci.*, **47**, 2818-2824.

Chen, T.-C. and J.-M. Chen, 1994: Low-Frequency Variations in Atmospheric Branch of the Global Hydrological Cycle. *J. of Clim.*, **8**, 92-107.

Chen, T.-C. and S.-P. Weng, 1999: Maintenance of Austral Summertime Upper-Tropospheric Circulation over Tropical South America: The Bolivian High-Nordeste Low System. *J. of Amtos. Sci.*, **56**, 2081-2100.

Chen, T.-C. 2002a: A North Pacific Short-Wave Train during the Extreme Phase of ENSO: *J. of Climate*, **15**, 2359-2376.

Chen, T.-C. 2002b: Maintenance of Summer Monsoon Circulation: A Planetary-Scale Perspective: *J. of Climate*, **16**, 2022-2037.

Chen, T.-C., M.-C. Yen, W.-R. Huang, and W. A. Gallus, 2002: An East Asian Cold Surge: Case Study. *Mon. Wea. Rev.*: **130**, 2271–2290.

Chen, T.-C., W.-R. Huang, and J.-H. Yoon, 2004: Interannual variation of the East-Asian Cold Surge Activity. *J. of Climate*: **17**, 401–413.

Chen, T.-C., 2004: The Structure and Maintenance of Stationary Waves in the Winter North Hemisphere. (Submitted)

Easterling, D. R., T. C. Peterson, and T. R. Karl, 1996: On the development and use of homogenized climate data set. *J. of Climate*, **9**, 1429-1434.

Gadgil, S., A. Guruprasad, and J. Srinivasan, 1992: Systematic bias in the NOAA outgoing longwave radiation datasets: *J. of Climate*: **5**, 867-875.

Gill, A. E., 1980: Some simple solution for heat-induced tropical circulation. *Q. J. R. Meteorol. Soc.*, **106**, 447-462.

Glantz, M. H. and M. Nakayama, 1998: ENSO event and impacts on Water Resources in South-East Asia, *Water Res. J.*, **197**, 87-92.

Holton, J. R. and D. E. Colton, 1972: A diagnostic study of the vorticity balance at 200mb in the tropics during the northern summer. *J. Atmos. Sci.*, **29**, 1124-1128.

Holton, J. R., 1992: An introduction to Dynamic Meteorology, 3rd, Academic Press, 381-383

Houze, R. A. Jr., S. G. Geotis, F. D. Marks. Jr., and A. K. West, 1981: Winter Monsoon Convection in the Vicinity of North Borneo. Part I: Structure and Time Variation of the Clouds and Precipitaion: *Mon. Wea. Rev.*, **109**, 1595-1614.

Hurrell, J. W., 1995: Transient Eddy Forcing of the Rotational Flow during Northern Winter: *J. Atmos. Sci.*, **52**, 2286-2301.

Johnson, R. H. and D. L. Priegnitz, 1981: Winter Monsoon Convection in the Vicinity of North Borneo. Part II: Effect on Large-Scale Fields: *Mon. Wea. Rev.*, **109**, 1615-1628.

Johnson, R. H. and D. C. Kriete, 1982a: Thermodynamic and Circulation Characteristics of Winter Monsoon Tropical Mesoscale Convection: *Mon. Wea. Rev.*, **110**, 1898-1911.

Johnson, R. H., 1982b: Vertical Motion in Near-Equatorial Winter Monsoon Convection: *J. of Meteor. Soc. of Japan*: **60**, 682–689.

Johnson, R. H., and R. A. Houze Jr., 1987: Precipitating Cloud Systems of the Asian

Monsoon. *Monsoon Meteorology,* ed. By C. P. Chang and K. M. W. Lau, Jonh Wiley & Sons (ISBN 0-471-87416-7), 298-353.

Kalnay, E., M. Kanamitsu, R. Kistler, W. Collins, D. Deaven, L. Gandin, M.Iredell, S. Saha, G. White, J. Woollen, Y. Zhu, M. Chelliah, W. Edisuzaki, W. Higgins, J. Janowiak, K. C. Mo, C. Ropelewski, J. Wang, A. Leetmaa, R. Reynolds, R. Jenne, and D. Joseph, 1996: The NCEP/NCAR 40-year reanalysis project. *Bull. Amer. Meteor. Soc.*, **77**, 473-471.

Kang, I.-S., and I. M. Held, 1986: Linear and nonlinear diagnostic models of stationary eddies in the upper troposphere during northern summer. *J. of Atmos. Sci.*, **43**, 3045-3057.

Krishnamurti, T. N., 1971: Tropical East-West Circulation During the Northern Summer, *J. of Atmos. Sci.*, **28**, 1342-1357.

Krishnamiriti, T. N., M. Kanamitsu, W. J. Koss and J. D. Lee, 1973: Tropical East-West Circulations During the Northern Winter, *J. of Atmos. Sci.*, **30**, 780-787.

Kanamitsu, M., W. Ebisuzaki, J. Woollen, S.-K. Yang, J. J. Hnilo, M. Fiorino and G. L. Potter, 2002: NCEP-DOE AMIP -II Reanalysis (R-2), *Bull. Amer. Meteor. Soc.*, **83**, 1631-1643.

Lau, K. M., and C.-P. Chang, 1983: Short-Term planetary-scale interactions over the tropics and mid-latitude during northern winter. Part II: Winter-MONEX periods. *Mon. Wea. Rev.*, **111**, 1372-1388.

Lau, K. M., and C.-P. Chang, 1987: Planetary Scale Aspects of the Winter Monsoon and Atmospheric Teleconnections: *Monsoon Meteorology,* ed. By C. P. Chang and K. M. W. Lau, Jonh Wiley & Sons (ISBN 0-471-87416-7), 161-202.

Lau, N. G., and M. J. Nath, 2000, Impacts of ENSO on the Variability of the Asian-Australian Monsoons as Simulated in GCM Experiments, *J. of Climate.*, **13**, 4287-4309.

Lim, T. K, 2002, Overvierw of Regional Climate Variability and ENSO's Influence on Reagional and Local Climate, *Asian Climate Training Manual*, Eds. By Neil etc., ASEAN Sub-Committee on Meteorology and Geophysics.

McBride, J. L., M. R. Haylock and N. Nicholls, 2003: Relationships between the Maritime Continent Heat Source and the El Niño-Southern Oscillation Phenomenon. *J. of Clim.*, **16**, 2905-2914

Nicholls, N., 1981: Air-Sea interaction and the possibility of long range weather prediction in the Indonesian Archipelago. *Mon. Wea. Rev.*, **109**, 2435-2443.

Peixoto, J. P. and A. H. Oort, 1983: The atmospheric branch of the hydrological cycle and climate. Variation in the Global Water Budget, A. Street-Perrottet al., Ed. Reidel, 5-65.

Peixoto, J. P. and A. H. Oort, 1991: Water Cycle: *Physics of Climate*: Springer (ISBN 0-88318-712-4), 270-307.

Pittock, B., B. Hunt, N. H. Tri, 2001: Climate Change and Variability, *Integrated Study Science Plan*, ed. By L. Label and W. Steffen, Southeast Asia Regional Committee for START.

Preedy, B. H., 1966: Far East Air Force Climatology. Headquarters, Far East Air Force, Singapore.

Rasmusson, E. M., 1972: Seasonal variation of tropical humidity parameters. *The General Circulation of the Tropical Atmosphere and Interactions with Extratropical Latitudes*. Vol. I, MIT Press.

Rasmusson, E. M. and T. H. Carpenter, 1983: The relationship between Eastern Equatorial Pacific Sea Surface Temperature and Rainfall over India and Sri Lanka. *Mon. Wea. Rev.*, **111**, 517-528.

Ramage., C. S.,1954: The cool-season tropical disturbances of Southeast Asia. *J. of Atmos.*. **12**. 252-262.

Ramage, C. S., 1968: Role of a Tropical "MARITIME CONTINENT" in the Atmospheric Circulation. *Mon. Wea. Rev.*: **96**, 365–370.

Ramage, C. S., 1971: March of the Seasons: *Monsoon Meteorolog*: Academic Press, 117-209.

Ropelewski, C. F., and M. S. Halpert, 1987: Global and Regional Scale Precipitation Patterns Associated with the El Niño/Southern Oscillation, *Mon. Wea. Rev.*, **115**, 1606-1626.

Rosen, R. D., D. A. Salstein andJ. P. Peixoto, 1979: Variability in the annual fields of large-scale atmospheric water vapor transport. *Mon. Wea. Rev.*, **107**,26-37

Salstein, D. A., R. D. Rosen and J. P. Peixoto, 1980: *Hemispheric watervapor fluxvariability-streamfunction andpotential fields. Atmospheric Water Vapor*, A. Deepak, T. D. Wilkerson andL. H. Ruhnke Eds., AcademicPress, 1980, 557-574

Streten, N. A., and J. W. Zillman, 1984: Climate of the South Pacific Ocean. *Climates of the Oceans*, H. van Loon, ed., World Survey of Climatology, **15**, 263-429.

Susskind, J., P. Piraino, L. Rokke, L. Iredell, and A. Mehta, 1997: Characterists of the TVOS Pathfinder Path A Datasets. *Bull. Amer. Meteor.*, **14**, 217-223.

Vose, R. S., R. L. Schmoyer, P. M. Steurer, T. C. Peterson, R. Heim, T. R. Karl, andJ. Eisheid, 1992: The Global Historical Climatological Network: long term monthlytemperature, precipitation, sea level pressure and station pressure data. ORNL/CDIAC-53, NDP-041, 325pp.Carbon Dioxide Information Analysis Center, Oak Ridge National Laboratory.

Simmons, A. J. and J. M. Wallace, 1983: Numerical Study of the Atmospheric Response to Equatorial Pacific Sea Surface Temperature Anomalies. *J. of Atmos. Sci.*, **40**, 1613-1630.

Yen, M.-C. and T.-C. Chen, 2002: A Revisit of the Tropical-midlatitude Interaction in East

Asia Caused by Cold Surges. *J. of Meteor. Soc. of Japan.*: **80**, 1115–1128.

Yoon, Jinho, 1999: Hydrological Cycle Associated with Monsoon Depressions: Master degree Thesis, Iowa State University, Ames, IA, U.S.A.

ACKNOWLEDGMENTS

First of all, sincere appreciation is extended to my major professor, Dr. Tsing-Chang Chen. His encouragement and support through the entire period made this work realized. I would like to express my gratitude to Drs. William A. Gallus, Jr. and S. Elwynn Taylor for serving on my committee. Their comments in improving this study are greatly appreciated, and I also express my gratitude to Dr. Ming-Cheng Yen at the National Central University in Taiwan for encouragement and support through the entire period of study.

During my graduate study, I was blessed, encouraged, and received a lot of help from my friend Shih-Yu Wang, Jinho Yoon, Judy Huang, Peter Hsieh, and David Li. Michael helped me to improve the manuscript. Editorial comments provided by Rebecca Shivvers are highly appreciated.

"*Cogito ergo sum*" René Descartes (1596-1650) claimed this formulation was the starting point of his philosophy in the 17th century. His works inspired the continental rationalism and provided a philosophical framework for the natural sciences as these began to develop.

This research was supported by NSF Grants ATM-9906454, ATM-0434798, and partially suported by Baker Endowment Fund 497-41-39-15-3803 AGRON ENDOW-D11-CHEN.